Open access • Journal Article • DOI:10.1029/94JD02688

Gravity wave activity in the lower atmosphere: Seasonal and latitudinal variations

Simon J. Allen, Robert A. Vincent

Published on: 20 Jan 1995 - Journal of Geophysical Research (John Wiley & Sons, Ltd)

Topics: Stratosphere, Tropopause, Troposphere, Gravity wave and Atmosphere

JOURNAL OF GEOPHYSICAL RESEARCH, VOL. 100, NO. D1, PAGES 1327–1350, JANUARY 20, 1995

Gravity wave activity in the lower atmosphere: Seasonal and latitudinal variations

Simon J. Allen and Robert A. Vincent
Department of Physics and Mathematical Physics, University of Adelaide, Adelaide, South Australia

Abstract. A climatology of gravity wave activity in the lower atmosphere based on high-resolution radiosonde measurements provided by the Australian Bureau of Meteorology is presented. These data are ideal for investigating gravity wave activity and its variation with position and time. Observations from 18 meteorological stations within Australia and Antarctica, covering a latitude range of 12°S – 68°S and a longitude range of 78°E – 159°E, are discussed. Vertical wavenumber power spectra of normalized temperature fluctuations are calculated within both the troposphere and the lower stratosphere and are compared with the predictions of current gravity wave saturation theories. Estimates of important model parameters such as the total gravity wave energy per unit mass are also presented. The vertical wavenumber power spectra are found to remain approximately invariant with time and geographic location with only one significant exception. Spectral amplitudes observed within the lower stratosphere are found to be consistent with theoretical expectations but the amplitudes observed within the troposphere are consistently larger than expected, often by as much as a factor of about 3. Seasonal variations of stratospheric wave energy per unit mass are identified with maxima occurring during the low-latitude wet season and during the midlatitude winter. These variations do not exceed a factor of about 2. Similar variations are not found in the troposphere where temperature fluctuations are likely to be contaminated by convection and inversions. The largest values of wave energy density are typically found near the tropopause.

1. Introduction

It is now well appreciated that gravity waves play a crucial role in determining the circulation and mean state of the atmosphere. If wave effects are to be fully understood and modeled then more information on the geographic and seasonal variations of wave activity and on wave sources is needed.

A wide variety of observational techniques have been used to study mesoscale fluctuations in the lower and middle atmospheres and their variations in time and space. These include balloon soundings [e.g., *Fritts et al.*, 1988; *Sidi et al.*, 1988; *Kitamura and Hirota*, 1989; *Cot and Barat*, 1990; *Tsuda et al.*, 1991], radar observations [e.g., *Tsuda et al.*, 1989; *Fritts et al.*, 1990], rocketsonde measurements [e.g., *Dewan et al.*, 1984; *Hamilton*, 1991; *Eckermann et al.*, 1994], and lidar studies [e.g., *Wilson et al.*, 1991; *Senft et al.*, 1993].

To date, much of our detailed knowledge of wave sources and effects in the lower atmosphere has come from ground-based wind-profiling radar studies [e.g., *Eckermann and Vincent*, 1993]. Instrumented commercial aircraft observations made in the troposphere and lower stratosphere during the Global Atmospheric Sampling Program also provided important information about wave fluxes over varying terrain and source regions [*Nastrom and Fritts*, 1992; *Fritts and Nastrom*, 1992]. While aircraft measurements provide coverage over both continental and oceanic regions, radar and lidar observations are primarily confined to land-based sites, except for a few ship-borne lidar measurements. Despite the excellent temporal resolution of the ground-based instruments it is unlikely that there will be sufficient numbers of such instruments deployed to enable wave climatologies to be established on a global scale, especially in the southern hemisphere.

Despite the large number of observational studies, certain theoretical questions remain unresolved. Initially, the debate was centered upon the relative importance of gravity waves as compared with two-dimensional turbulence in forming the fluctuations observed in the atmosphere. *Dewan* [1979] and *VanZandt* [1982] argued for a gravity wave interpretation, suggesting that mesoscale fluctuations are the direct result of a superposition of many gravity waves. However, *Gage* [1979], *Lilly* [1983], and *Gage and Nastrom* [1985] argued that two-dimensional turbulence is the main cause of mesoscale fluctuations. It is likely that both waves and stratified turbulence are present in the atmosphere,

Paper number 94JD02688.
0148-0227/95/94JD-02688$05.00

although it is now widely accepted that gravity wave motions are dominant [e.g., *Vincent and Eckermann*, 1990].

Recently, debate has focused upon the physical process apparently acting to limit wave amplitude growth with height. A common feature of many experimental studies is approximately invariant vertical wavenumber and frequency power spectra, despite the exponential decrease of density with height, and regardless of season and geographic location. This feature, first recognized by *VanZandt* [1982] and based on similar studies of oceanic gravity wave power spectra, led to the concept of a "universal" spectrum of atmospheric gravity waves with amplitudes constrained to remain below some fixed value. Several saturation theories have since emerged [*Dewan and Good*, 1986; *Smith et al.*, 1987; *Weinstock*, 1990; *Hines*, 1991].

Each theory proposes a physical mechanism thought to be responsible for limiting wave amplitude growth and each predicts, approximately, the saturated vertical wavenumber power spectrum amplitudes that should be observed. However, due to theoretical uncertainties in the various proposed mechanisms, it has proven difficult to distinguish between them on the basis of spectral amplitude calculations alone. The question of which physical mechanism is acting at high vertical wavenumbers is still, very much, an open one. It seems likely that the successful theory will best account for some of the more unusual experimental findings such as recent lidar measurements within the stratosphere [*Hines*, 1993].

Very recently, *Fritts and VanZandt* [1993] and *Fritts and Lu* [1993] developed a gravity wave parameterization scheme which describes the influence of a broad spectrum of waves on the mean state of the atmosphere. The scheme is based on the concept of a "universal" spectrum which is separable in frequency and vertical wavenumber. Only a few parameters are required to constrain this model and the scheme links the work of theorists, who model large-scale motions in the atmosphere, and experimentalists who use convenient analytical tools such as power spectrum analysis. However, the extent to which wave activity and influence varies with height, season, and geographic location is poorly understood at present. Despite the constraining influence of the proposed saturation theories there still exists the possibility for significant variations in the wave field, both at low vertical wavenumbers and, in some instances, at high vertical wavenumbers also. Quantifying these variations is an important experimental problem.

Balloon-borne radiosonde soundings provide one potentially important source of information on gravity waves and their effects in the troposphere and lower stratosphere. Early work by, for example, *Sawyer* [1961] and *Thompson* [1978] provided evidence for large-scale inertial waves in the lower stratosphere and more recently, *Kitamura and Hirota* [1989] emphasized the importance of radiosonde observations in their study of inertial-scale disturbances over Japan. Radiosonde soundings are carried out daily on a world-wide basis, providing a wealth of information on winds, temperatures, and humidity. One reason why radiosonde measurements have been little used in wave studies is that measurements are reported and archived at relatively infrequent height intervals, leading to poor height resolution. Recently, however, the Australian Bureau of Meteorology began routinely recording and archiving high-resolution data from radiosondes, with pressure, temperature and relative humidity measurements made every 10 s, or about 50 m in altitude. These data are ideal for investigations of wave energies and power spectra in the troposphere and lower stratosphere.

The Australian soundings are taken once or twice per day from stations whose locations vary from the tropics to the Antarctic. The observations also cover a significant spread of longitudes in the Australian sector. By suitably combining measurements made at a range of longitudes in relatively narrow latitude bands it is possible to build up a climatology of wave activity which is not biased by localized source effects, such as topography. Here we explore the extent to which this extensive data set of high-resolution radiosonde measurements can contribute to solving some of the problems described above.

Section 2 of this paper details some background theory as well as discussing the state of current saturation models of temperature fluctuation spectra. In section 3 the radiosonde data set that was used, the analysis procedures that were employed, and the possible sources of measurement errors are described. Vertical wavenumber power spectra of normalized temperature fluctuations are presented in section 4 as are estimates of the total gravity wave energy density, E_0, which is an important component of the *Fritts and VanZandt* [1993] parameterization scheme. A discussion of the results is given in section 5 followed by the conclusions in section 6. The consequences of radiosonde temperature-sensor response time with regards to measurement accuracy are described in an appendix.

2. Gravity Wave Power Spectra Theory

Fritts and VanZandt [1993] (hereinafter referred to as FV93) presented a model three-dimensional gravity wave power spectrum which makes use of functional forms of the one-dimensional vertical wavenumber and frequency power spectra that are in good agreement with experimental findings. They assumed a total energy spectrum that is separable in vertical wavenumber, m, intrinsic frequency, ω, and azimuthal direction of propagation, ϕ, and is given by

$$E(\mu,\omega,\phi) = E_0 A(\mu) B(\omega) \Phi(\phi) \tag{1}$$

where

$$A(\mu) = A_0 \mu^s / \left(1 + \mu^{s+t}\right) \tag{2}$$

$$B(\omega) = B_0 \omega^{-p} \tag{3}$$

and where $\mu = m/m_*$, $m = 2\pi/\lambda_z$, λ_z is the vertical wavelength, m_* is the characteristic wavenumber (in units of radians per second), E_0 is the total gravity

wave energy per unit mass (energy density), A_0 and B_0 are defined by the normalization constraints of $A(\mu)$ and $B(\omega)$, the function $\Phi(\phi)$ contains the dependence on wave field anisotropy and the parameters s, t, and p are to be determined by comparison with the slopes of observed power spectra.

The quantity E_0, an important parameter of the FV93 formulation, is chosen in this paper as the measure for gravity wave activity. It is defined by

$$E_0 = \frac{1}{2}\left[\overline{u'^2} + \overline{v'^2} + \overline{w'^2} + \frac{g^2\overline{\hat{T}'^2}}{N^2}\right] \tag{4}$$

where u', v', and w' are the zonal, meridional, and vertical components of first-order wind velocity perturbations, respectively, g is the acceleration due to gravity, N is the Vaisala-Brunt frequency, $\hat{T}' = T'/\overline{T}$ is the normalized temperature fluctuation, and $\overline{T}$ and T' are the background and first-order perturbation of atmosphere temperature, respectively. Strictly, measurements of three component wind velocity and temperature are required to completely define E_0. However, it is possible to estimate this parameter from temperature measurements alone by making use of the appropriate gravity wave polarization equation and the three-dimensional model spectrum of FV93. This arises since u', v', w', and $\hat{T}'$ are all coupled to each other through gravity wave polarization equations.

Consider the equation relating the three-dimensional power spectrum of normalized temperature fluctuations to that of total energy,

$$E_{\hat{T}'}(\mu,\omega,\phi) = \frac{N^2}{g^2}\frac{(1-f^2/\omega^2)}{(1-f^2/N^2)}E(\mu,\omega,\phi) \tag{5}$$

where f is the inertial frequency. This follows from the equations presented by FV93 which in turn can be derived from standard textbook formulations of the polarization equations, at least those involving the Boussinesq approximation [e.g., *Gossard and Hooke*, 1975]. By integrating both sides of (5) with respect to μ, ω, and ϕ using (1), (2), (3), and the normalization condition for $\Phi(\phi)$, namely, $\int_0^{2\pi}\Phi(\phi)d\phi = 1$, the following equation is derived relating the energy density E_0 to the total normalized temperature variance,

$$E_0 = \frac{g^2}{N^2}\frac{1}{B_0 C_{In}}\overline{\hat{T}'^2} \tag{6}$$

where

$$C_{In} = \frac{f^{1-p}}{1-\tilde{f}^2}\left[\frac{1-\tilde{f}^{p-1}}{p-1} - \frac{1-\tilde{f}^{p+1}}{p+1}\right] \tag{7}$$

and where $\tilde{f} = f/N$, p is the slope of the one-dimensional frequency spectrum, and B_0 is given by FV93. The best estimate of p from the literature is 5/3 and this value will be assumed hereinafter. In obtaining (6), three assumptions have been made: first, the three-dimensional energy spectrum is assumed to be separable in m, ω, and ϕ; second, the one-dimensional frequency spectrum is assumed to be of the form $B(\omega) \propto \omega^{-p}$ where p is 5/3; third, the Boussinesq approximation is assumed valid since this is used in obtaining (5). The normalized temperature variance from a given height interval is easily measured, and (6) will be used in a later section to calculate the gravity wave energy density.

A more typical analysis of radiosonde temperature measurements involves calculating vertical wavenumber power spectra of normalized temperature fluctuations. These, together with results derived from other experimental techniques, provide a good picture as to the nature and shape of vertical wavenumber gravity wave fluctuation spectra. Generally, a high-wavenumber "tail" region, displaying a -3 power law form and having approximately invariant spectral amplitudes, is observed and this is separated from the low-wavenumber source-dependent region by the so-called characteristic wavenumber m_*. Spectral amplitudes in the low-wavenumber region can increase with height but must do so in accordance with wave action conservation. The typical observed shape is well represented by the modified-Desaubies form, $A(\mu)$, first introduced by *VanZandt and Fritts* [1989].

The spectral amplitudes of the high wavenumber "tail" region have been predicted by several authors on the basis of the physical mechanism thought most important in causing gravity waves to saturate. When theoretical uncertainties are taken into consideration, however, these predictions are difficult to differentiate, and for the purposes of this paper the saturation limit of *Smith et al.* [1987] will be used as a convenient reference. This limit is given below for the power spectral density of normalized temperature fluctuations as a function of inverse vertical wavelength,

$$E_{\hat{T}'}(1/\lambda_z) \approx \frac{N^4}{6g^2}\frac{1}{p}\frac{1}{(2\pi)^2}\frac{1}{(1/\lambda_z)^3} \tag{8}$$

where λ_z is the vertical wavelength and, as before, p is the slope of the one-dimensional frequency spectrum. In their original paper, *Smith et al.* [1987] derived the saturation limit for the specific case of a one-dimensional vertical wavenumber power spectrum of total horizontal wind velocity, which was assumed to take the form defined by (2) with $s = 0$ and $t = 3$. Equation (8) follows from this using a suitable polarization equation and assuming that the one-dimensional frequency spectrum is given by $B(\omega) \propto \omega^{-p}$ [see *Fritts et al.*, 1988].

The purpose of spectral analysis in this paper is not so much to confirm the agreement between theory and experiment, something that appears to have been accepted already, but rather to study how the shape and amplitudes of vertical wavenumber power spectra can vary with geographic position and time. The extent of these variations is not well known at present and the available data set of high-resolution radiosonde measurements is ideal for addressing the problem. Details of the experimental data that were used are provided in the following section.

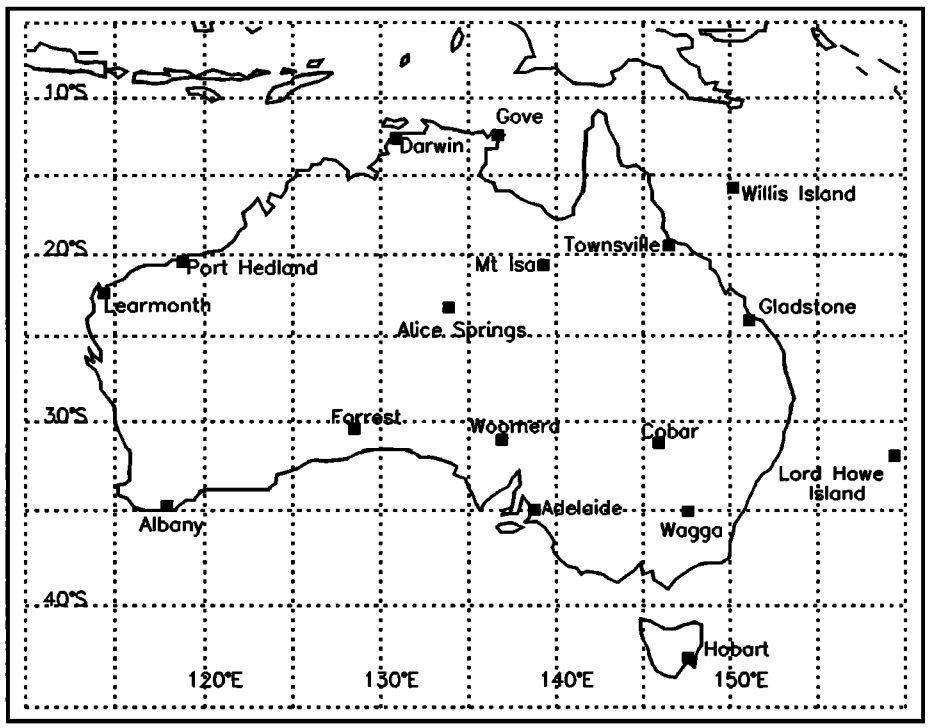

Figure 1. The geographic distribution of radiosonde stations used in the study. Davis (69°S, 78°E), in Antarctica, is not shown.

3. Experimental Data and Analysis Procedures

Radiosonde Measurements

The Australian Bureau of Meteorology launches one or two radiosondes per day from 36 meteorological stations and has recently begun archiving these measurements. Observations from 18 stations have been chosen for use in this study and these are shown, with the exception of Davis (69°S, 78°E), in Figure 1. Pressure, temperature, and relative humidity measurements are recorded at 10-s intervals which correspond, approximately, to 50-m altitude intervals. Data were available for at least a 1-year period (June 1991 to May 1992) from all but two of the stations, Davis and Willis Island. Only 10 months of data were available from these sites.

Each meteorological station in Figure 1 makes use of radiosondes manufactured by Vaisala Oy and the data obtained were subjected to quality control procedures developed by that company. These procedures include removing suspect measurements and replacing them by linear interpolation. A measurement is deemed to be suspect if it does not satisfy certain rejection criteria based on known physical constraints. In addition, the raw measurements, made at approximately 2-s intervals, are smoothed in order to obtain the 10-s "filtered" data that are used here.

Temperature measurements are of particular interest in this study. Figure 2 displays examples of temperature profiles observed by radiosondes launched from Darwin (12°S, 131°E) and Davis (69°S, 78°E) during the months of January and July. These examples are chosen because of their extreme natures. The tropopause over Darwin is typically found near 16 km, whereas the same level over Davis occurs, on average, at about 9 km. Typical tropopause levels from other locations tend to fall between these heights. Notice that successive profiles, corresponding to a 12-hour delay between soundings, have been displaced by 10°C. The data obtained from other stations were not always at 12-hour intervals, as indicated by these examples. From many stations, measurements from only one sounding per day were available.

Vertical Wavenumber Power Spectrum Analysis

Radiosonde profiles of normalized temperature fluctuations, $\hat{T}'$, were spectrally analyzed in two altitude intervals, usually between 2.0 and 9.0 km in the troposphere and 17.0 and 24.0 km in the stratosphere. However, at some stations slightly different height ranges were used and these are listed in Table 1. Notice also the shaded regions of Figure 2 which correspond to the particular intervals used for the analysis of observations made at Davis and Darwin. The principal reason for choosing these ranges was to ensure a stationary power spectrum since, according to theory, the vertical wavenumber power spectrum of normalized temperature fluctuations is dependent upon N^4. Therefore height regions in which the Vaisala-Brunt frequency is approximately constant should be used.

Data segments for which continuous measurements were unavailable throughout the entire height interval

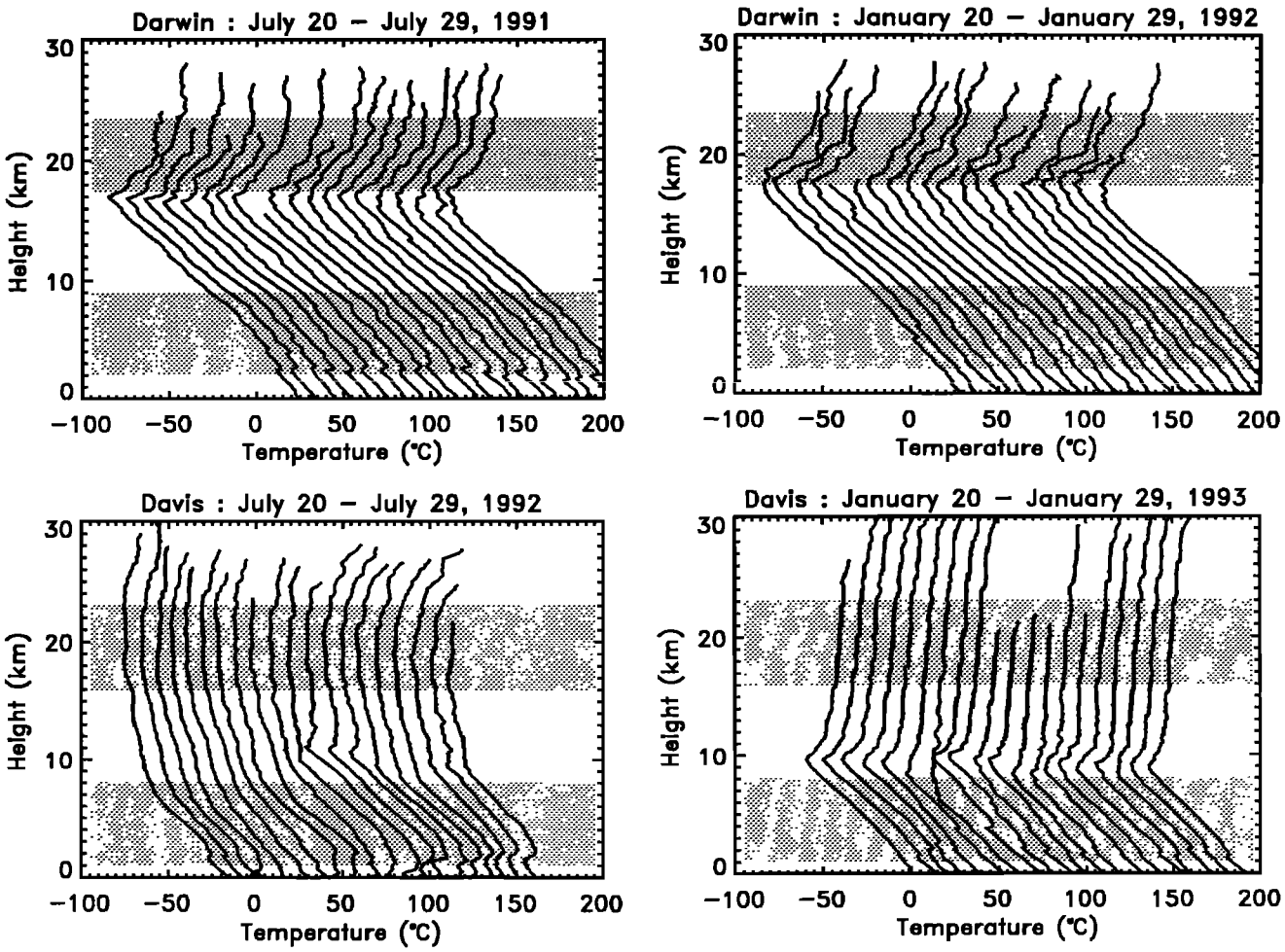

Figure 2. Examples of temperature profiles observed at Darwin (12°S, 131°E) and Davis (69°S, 78°E) during the months of January and July. Radiosondes were launched at 12-hour intervals during these periods. Successive profiles are displaced by 10°C, and the shaded areas correspond to the height ranges for which temperature profiles were spectrally analyzed.

of interest or for which a tropopause was found within this interval were not included in the power spectrum analysis. The former condition often arose when the sonde did not reach the maximum height required for a given station as defined in Table 1. The latter condition also arose from time to time and the relevant profiles were excluded to ensure a constant background Vaisala-Brunt frequency profile. Approximately 30% of all available stratospheric data segments were rejected in this manner. This figure, however, was much smaller for tropospheric data. The particular height ranges that were employed at each station were chosen in order to minimize the number of profiles rejected.

Normalized temperature fluctuation profiles were calculated by estimating $\overline{T}$ with a fitted second-order polynomial over the particular height interval being investigated. These were then spectrally analyzed using the Blackman-Tukey algorithm with a 90% lag Bartlett window where the data points were first prewhitened by differencing. The technique follows *Dewan et al.* [1984] who used the same algorithm to analyze horizontal wind velocity fluctuations derived from rocket-laid vertical smoke trails.

The vertical wavenumber power spectra calculated from individual temperature profiles were then averaged in order to improve the confidence limits of spectral amplitude estimates. Following the suggestion of T. E. VanZandt (private communication, 1992), normalized individual power spectra were averaged, that is, each spectrum was divided by its total variance before averaging. The purpose of this technique was to ensure that all spectra contribute equally to the shape of the mean spectrum. Once calculated, the mean spectrum was renormalized by multiplying by the averaged total variance.

A possible source of error in the analysis procedure arises due to the fact that radiosonde observations are unequally spaced in altitude. Although successive measurements were recorded at 10-s intervals, the corresponding altitudes traversed by the sonde tended to vary; typical height intervals were found to be between 40 and 60 m. Strictly speaking, the Blackman-Tukey

Table 1. Information Concerning the Radiosonde Data Used in the Study

Station Name	WMO Station Number	Location deg South, deg East	Height Intervals for Data Analysis, km		Time Intervals	Total Number of Available Soundings	Number of Soundings Analyzed	
			Troposphere	Stratosphere			Troposphere	Stratosphere
Adelaide	94672	35.0, 138.5	2.0–9.0	17.0–24.0	May 1991 – Feb. 1993	1344	1224	909
Albany	94802	35.0, 117.5	2.0–9.0	17.0–24.0	March 1991 – May 1992	519	481	364
Alice Springs	94326	23.4, 133.5	2.0–9.0	17.0–24.0	May 1991 – May 1992	366	336	244
Cobar	94711	31.3, 145.5	2.0–9.0	17.0–24.0	April 1991 – May 1992	528	498	373
Darwin	94120	12.2, 130.5	2.0–9.0	17.5–23.5	June 1991 – May 1992	730	655	453
Davis	89571	68.6, 78.0	1.0–8.0	16.0–23.0	July 1992 – April 1993	556	481	435
Forrest	94646	30.5, 128.1	2.0–9.0	17.0–24.0	April 1991 – May 1992	421	402	343
Gladstone	94380	23.5, 151.2	2.0–9.0	17.0–24.0	June 1991 – May 1992	435	408	263
Gove	94150	12.2, 136.5	2.0–9.0	17.5–24.5	June 1991 – May 1992	457	431	313
Hobart	94975	42.5, 147.2	2.0–9.0	16.0–23.0	April 1991 – May 1992	852	799	452
Learmonth	94302	22.1, 114.0	2.0–9.0	17.0–24.0	June 1991 – May 1992	348	339	239
Lord Howe Island	94995	32, 159	2.0–9.0	17.0–24.0	June 1991 – May 1992	444	401	287
Mount Isa	94332	20.4, 139.3	2.0–9.0	17.0–24.0	April 1991 – May 1992	575	520	350
Port Hedland	94312	20.2, 118.4	2.0–9.0	18.0–25.0	Nov. 1990 – May 1992	531	519	474
Townsville	94292	19.2, 146.5	2.0–9.0	17.0–24.0	June 1991 – May 1992	341	334	234
Wagga	94910	35.1, 147.2	2.0–9.0	17.0–24.0	May 1991 – May 1992	485	447	331
Willis Island	94299	16, 150	2.0–9.0	17.5–24.5	Aug. 1991 – May 1992	304	286	249
Woomera	94659	31.1, 136.5	2.0–9.0	17.0–24.0	April 1991 – May 1992	544	505	393

algorithm cannot be applied to unequally spaced data such as this.

The approach used here was to interpolate the measurements at 50-m intervals using cubic spline interpolation and to assume that the calculated power spectrum was not significantly different from the spectrum that would be found were the original data points equally spaced. In order to be confident of this, however, a comparison was made between vertical wavenumber power spectra of radiosonde normalized temperature fluctuations calculated with both the Blackman-Tukey algorithm and with a particular discrete Fourier transform. This latter technique was proposed by *Ferraz-Mello* [1981] and was devised specifically for the purposes of making accurate estimates of power spectral density from unequally spaced data. The comparison was found to be very favorable and so the Blackman-Tukey algorithm appears to have valid application in this case.

A further source of error for vertical wavenumber power spectral density calculations from radiosonde temperature data arises from the nature of balloon observations. Instrumented balloons rise slowly in the vertical at speeds of approximately 5 m s^{-1} and also drift horizontally with the background winds. As a consequence, any observed power spectra are not strictly vertical wavenumber power spectra since the observations are not made simultaneously in time, nor are they obtained along a vertical line from the point of the balloon's release. *Sidi et al.* [1988] and *Gardner and Gardner* [1993] have considered this problem for radiosonde measurements of a broad spectrum of predominantly saturated gravity waves. Both studies suggest that any errors introduced to the vertical wavenumber power spectrum estimates are usually negligible. *Gardner and Gardner* [1993] did, however, conclude that nonnegligible distortion may be possible when horizontal wind speeds reach approximately 60 m s^{-1} or larger. Nevertheless, for the data used here, it is argued that even this distortion is small when compared with the much greater distortion caused by the relatively slow response of the radiosonde's temperature sensor at stratospheric heights. The response time is peculiar to the type of sensor used and, if large enough, will prevent the radiosonde from accurately measuring rapid changes in temperature as the balloon moves vertically. The measured power spectra can, however, be corrected and this correction procedure will now be discussed.

Radiosonde Instrumental Response

It is well known that a temperature sensor will behave in such a way that the rate of change of the sensor's temperature is proportional to the difference between the temperature of the sensor and that of its surrounding environment [*Fritschen and Gay*, 1979]. Mathematically, this may be expressed as

$$\frac{dT_s}{dt} = -\frac{1}{\tau}\,[T_s - T] \tag{9}$$

where T_s is the sensor temperature, T is the environment temperature, and τ is defined as the response time constant. The value of τ is peculiar to the type of sensor used and to the environment in which it is placed.

The response of a given temperature sensor to any time-varying environment temperature $T(t)$ is completely defined by (9). The steady state response to a sinusoidally varying environment is of particular importance, however, since this describes a filter function, $I(\omega)$, which relates the environment or input spectrum $X(\omega)$ to the measured spectrum $X_s(\omega)$ according to $X_s(\omega) = I(\omega)X(\omega)$ at each angular frequency ω [e.g., *Bath*, 1974]. Here $X(\omega)$ and $X_s(\omega)$ refer to the Fourier transforms of $T_s(t)$ and $T(t)$, respectively, rather than their power spectral densities. If $I(\omega)$ is known then the environment spectrum can be recovered from the observed spectrum since $X(\omega) = X_s(\omega)/I(\omega)$.

Consider the case of a balloon which rises at constant vertical velocity V_0 and carries a temperature sensor with known response time τ. Suppose also that the sensor is measuring a background or environment temperature profile that is sinusoidally dependent upon height z but is independent of time, that is, $T(z) = A\exp[i(mz + \phi)]$ where $m = 2\pi/\lambda_z$ and where the complex notation has its usual meaning. Equation (9) is therefore given by

$$\frac{dT_s}{dz} + \frac{1}{\beta}\,T_s = \frac{1}{\beta}\,T \tag{10}$$

where $\beta = V_0\tau$. The "steady state" solution of this new equation for constant β is readily calculated,

$$T_s(z) = \frac{A}{1 + im\beta}\exp[i(mz + \phi)] \tag{11}$$

and thus defines a filter function $I(m) = 1/[1 + im\beta]$, analogous to the function $I(\omega)$ discussed earlier, which relates the Fourier transform of $T_s(z)$ to that of $T(z)$ at each spatial frequency or wavenumber m. Since power spectral density is simply the absolute value squared of a Fourier transform it follows that the observed vertical wavenumber power spectrum is related to the true or environment power spectrum according to the following equation

$$E_{T_s}(m) = \frac{1}{1 + (m\beta)^2}\,E_T(m) \tag{12}$$

where $E_{T_s}(m)$ and $E_T(m)$ are vertical wavenumber power spectra of $T_s(z)$ and $T(z)$ fluctuations respectively. Equation (12) can therefore be used to correct observed vertical wavenumber power spectra of temperature fluctuations and to recover their true forms provided that V_0 and τ are known and are constants. Furthermore, the relation is also valid for vertical wavenumber power spectra of normalized temperature fluctuations provided that $\overline{T_s}(z)$ does not differ significantly from $\overline{T}(z)$. We believe that this is a reasonable assumption.

Figure 3 displays the measurement distortion of a modified-Desaubies vertical wavenumber power spectrum with $m_*/2\pi = 5 \times 10^{-4}$ cycles per meter and with

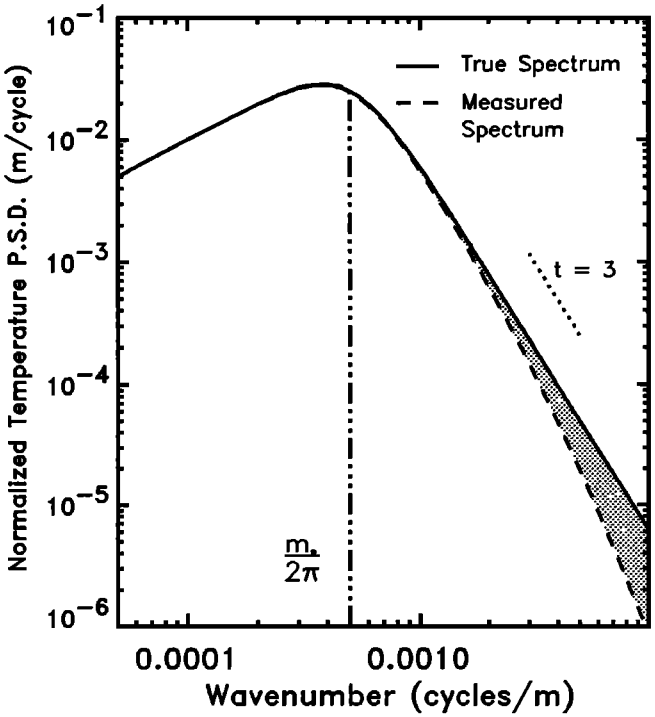

Figure 3. The theoretical distortion of a modified-Desaubies vertical wavenumber power spectrum measured by a radiosonde with temperature sensor response time $\tau = 8$ s and with vertical ascent velocity $V_0 = 5$ m s^{-1}. The shaded region comprises 4% of the total area under the modified-Desaubies spectrum.

spectral amplitudes chosen to represent typical observations of normalized temperature fluctuations. The parameter β was assigned the value of 40 m. This corresponds to the typical balloon ascent velocity ($V_0 = 5$ m s^{-1}) and to estimates of response times ($\tau = 8$ s) within the altitude range 17–24 km. Notice that the spectral distortion is only significant at high vertical wavenumbers. Notice also that the total observed variance is not significantly reduced since the shaded area of Figure 3 comprises just 4% of the total area under the modified-Desaubies spectrum.

Estimating the radiosonde's temperature sensor response time poses a difficult problem since τ depends upon air temperature and air density. A broad discussion of how these estimates can be obtained and to what extent they are reliable is given in the appendix. The discussion is based on experimental results presented in two Vaisala Oy test reports. However, it should be noted here that there is some uncertainty as to the correct value for the response time τ. This may result in a bias for the spectral parameter, t, of corrected power spectra, although estimates of both the characteristic wavenumber and the total wave variance will not be significantly affected. More details are provided in the appendix.

The height-averaged response times were found to lie between 7 and 8 s within the 17 to 24-km altitude range and between 1 and 2 s within the 2 to 9-km altitude range. The response times were not constant within these ranges but may be considered as constants to good approximation. This point is discussed further in the appendix and is not believed to result in serious errors, despite the fact that τ was assumed to be constant in the derivation of (12). Since the response time is small within the troposphere, the correction to the observed power spectrum, for the wavenumber range that is being investigated here, is marginal. As a result the correction technique will only be applied to stratosphere power spectra.

In Figure 4 the mean vertical wavenumber power spectra of normalized temperature fluctuations observed at Adelaide (35°S, 139°E) for both summer and winter months within the altitude range 17–24 km are presented. Also plotted are the corrected power spectra, as defined by (12), where τ was obtained using the technique described in the appendix and where an average V_0 was used since the balloon ascent velocity is known for each individual temperature profile. We believe that the corrected spectrum provides the best estimate of the true normalized temperature power spectral density. All of the stratosphere power spectra that are presented and discussed in the following sections will have undergone this correction procedure.

4. Power Spectra and Energy Density Variations

Vertical wavenumber power spectra of normalized temperature fluctuations within the troposphere and lower stratosphere are presented in this section. Figure 5 displays seasonally averaged spectra from three different stations (Gove, Adelaide, and Hobart) which were chosen to represent low-latitude and midlatitude sites. The seasonally averaged spectra from other locations, with the exception of Davis, were found to be similar to these. Figure 6 displays time and zonally averaged vertical wavenumber power spectra. These were obtained by averaging spectra from each station into seven latitude bands as described in Table 2. The purpose of presenting the spectra in this manner is to look for seasonal and latitudinal variations of the gravity wave spectral form.

Each power spectrum of Figures 5 and 6 has been presented with a maximum wavenumber of 8.0×10^{-3} cycles per meter. However, the Nyquist spatial frequency for data interpolated at 50-m altitude intervals is 0.01 cycles per meter. The cutoff wavenumber was chosen since the mean separation of adjacent points for a given temperature profile was found to vary about 50 m. As a consequence, spectral amplitudes at the very highest wavenumbers may be biased due to aliasing.

Seasonal variations of the gravity wave spectral form are difficult to observe in the spectra of Figure 5, confirming the "universal" nature of the gravity wave field. Small variations can be seen but are most noticeable within the low-wavenumber, source-dependent, region of the spectrum, as might be expected. For example, the winter months at Adelaide and Hobart are charac-

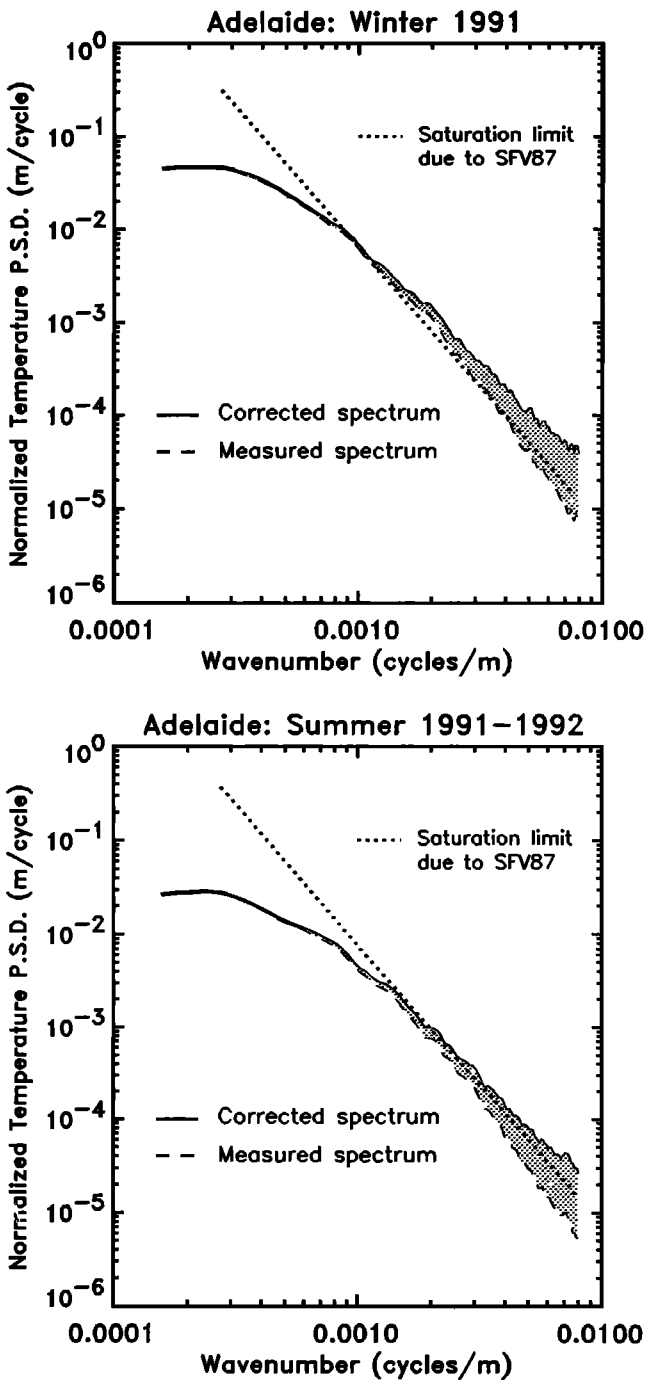

Figure 4. The mean vertical wavenumber power spectra of normalized temperature fluctuations (dashed lines) observed at Adelaide (35°S, 139°E) for both summer and winter months. All spectra were calculated within the 17–24 km altitude range. Also plotted are the corrected spectra (solid lines), where the correction technique is described in the text, and the theoretical saturation limits of *Smith et al.* [1987] (denoted by SFV87). The shaded regions comprise approximately 5% of the total area under each corrected spectrum.

terized by an increase in frontal activity at ground level. Since cold fronts are known gravity wave sources [*Eckermann and Vincent*, 1993], it is plausible to suppose that the source-dependent region of the spectrum will display larger amplitudes during winter than during summer. Also *Kitamura and Hirota* [1989] have suggested a relationship between wave disturbances and the subtropical jet at the tropopause level which peaks during winter months. We do observe larger spectral amplitudes during winter and within the low-wavenumber region of the spectrum at stratospheric heights but this is much less obvious within the troposphere. The opposite should be true at low-latitude sites, such as Gove, where increased source spectrum activity is expected during the monsoon season (December to February). The observed spectra within the stratosphere do show slightly larger amplitudes during this period and within the source-dependent region, but surprisingly this is not the case at tropospheric heights where larger spectral amplitudes are found during the dry season.

Latitudinal variations of the gravity wave spectral form (Figure 6) are generally not significant, although the stratosphere power spectrum observed at Davis (latitude band 7) is an exception. This shows smaller spectral amplitudes and a shallower slope than is expected theoretically and in comparison with the spectra observed at other latitudes. Curiously, the troposphere and stratosphere power spectra are very similar in this case, despite the significant increase of atmosphere stability near the tropopause.

The power spectra of Figures 5 and 6 confirm the approximate invariance of the gravity wave field with time and geographic location. However, the stratosphere power spectrum observed at Davis is an exception. Nevertheless, all other stations, which are located near a range of different geographic features, show remarkably similar spectra within both the troposphere and the lower stratosphere. Most are not shown here for the purpose of brevity, although each station, with the exception of Willis Island, has contributed to the spectra that are presented in Figure 6. The invariance of the spectral form occurs despite, what are assumed to be, large differences in the source spectrum of waves at each different location.

Table 3 presents estimates of the spectral parameters E_0, t, $m_*/2\pi$, and $c_* = N/m_*$, which are all defined within the FV93 model formulation. These are determined from the shape and spectral amplitudes of the observed spectra at each station. The estimates of E_0 were obtained using (6) and (7) where $\overline{\hat{T}'^2}$ is simply the area under the relevant power spectrum and where an averaged Vaisala-Brunt frequency, N, was used. Estimates of t and $m_*/2\pi$, and hence c_* also, were found using the Levenberg-Marquardt least squares curve-fitting algorithm with a fitting function given below.

$$F(m) = F_0 \frac{m/m_*}{1+(m/m_*)^{t+1}} \tag{13}$$

The three unknown parameters, F_0, m_*, and t, were obtained by fitting to monthly mean spectra and then averaging these estimates over all time. Table 3 provides a description, at least to a certain extent, of the mean behavior of the gravity wave field at each station. However, other important parameters, such as the wave

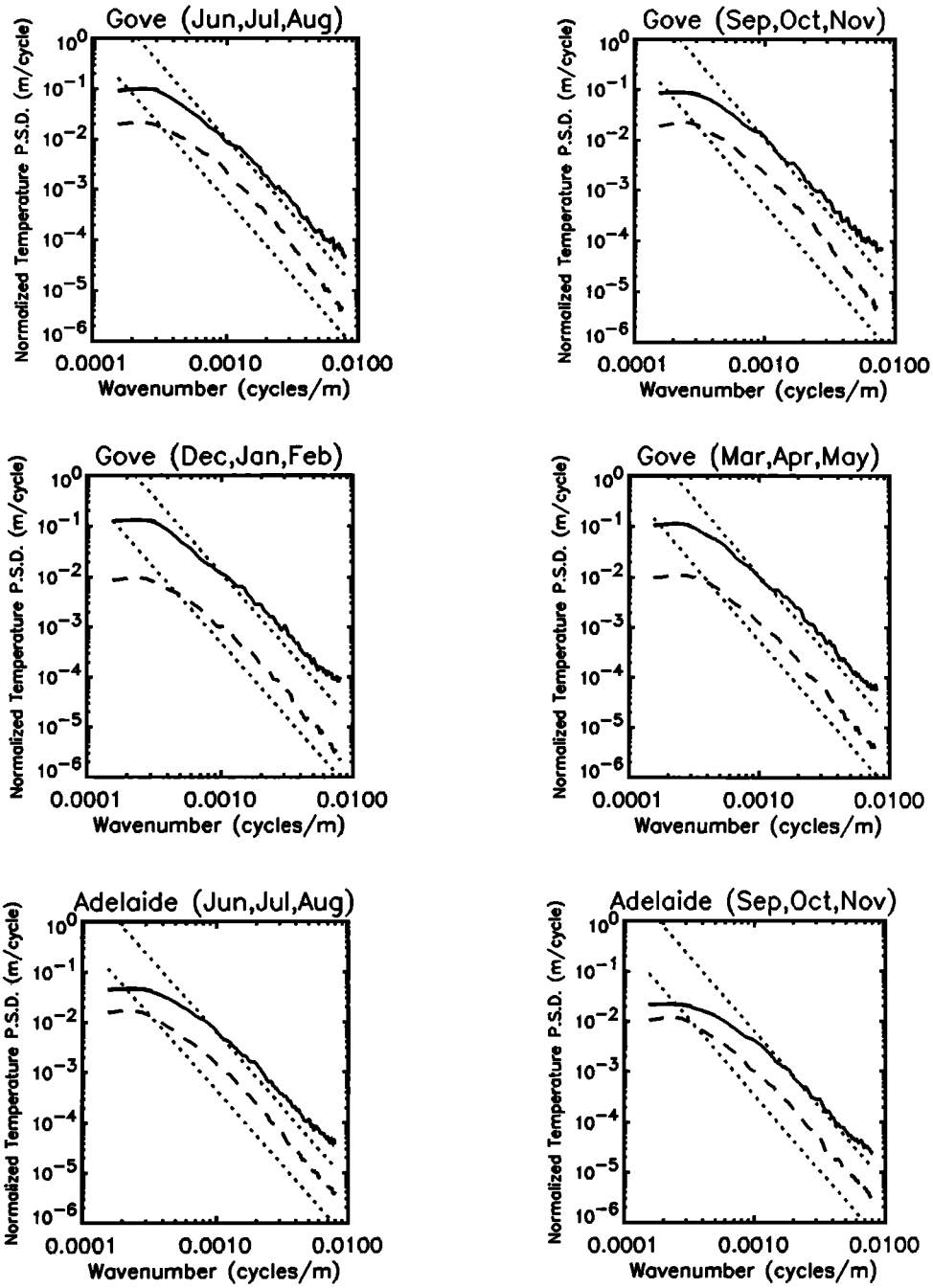

Figure 5. Vertical wavenumber power spectra of normalized temperature fluctuations for the troposphere (dashed lines) and lower stratosphere (solid lines). The theoretical saturation limits of *Smith et al.* [1987] are also plotted for comparison purposes (dotted lines). Each spectrum is a 3-month average, and results from Gove, Adelaide, and Hobart are presented. The 95% confidence limits are approximately given by 0.85 and 1.15 multiplied by the spectral amplitude at each wavenumber.

field anisotropy, cannot be estimated from radiosonde temperature measurements alone.

The spectral parameter, t, for stratosphere power spectra was found to be consistently smaller than 3, the expected value from linear saturation theory. However, this parameter for troposphere power spectra was found to be very close to 3 at most stations. Recall that each stratospheric power spectrum has been corrected for spectral distortion that is believed to be associated with the radiosonde's temperature sensor response time. The troposphere power spectra have not undergone this correction procedure, however, since the response time is small at tropospheric heights. It is possible that estimates of t within the stratosphere are biased since there is some uncertainty as to the correct value for τ. As a consequence, all values within the relevant column of

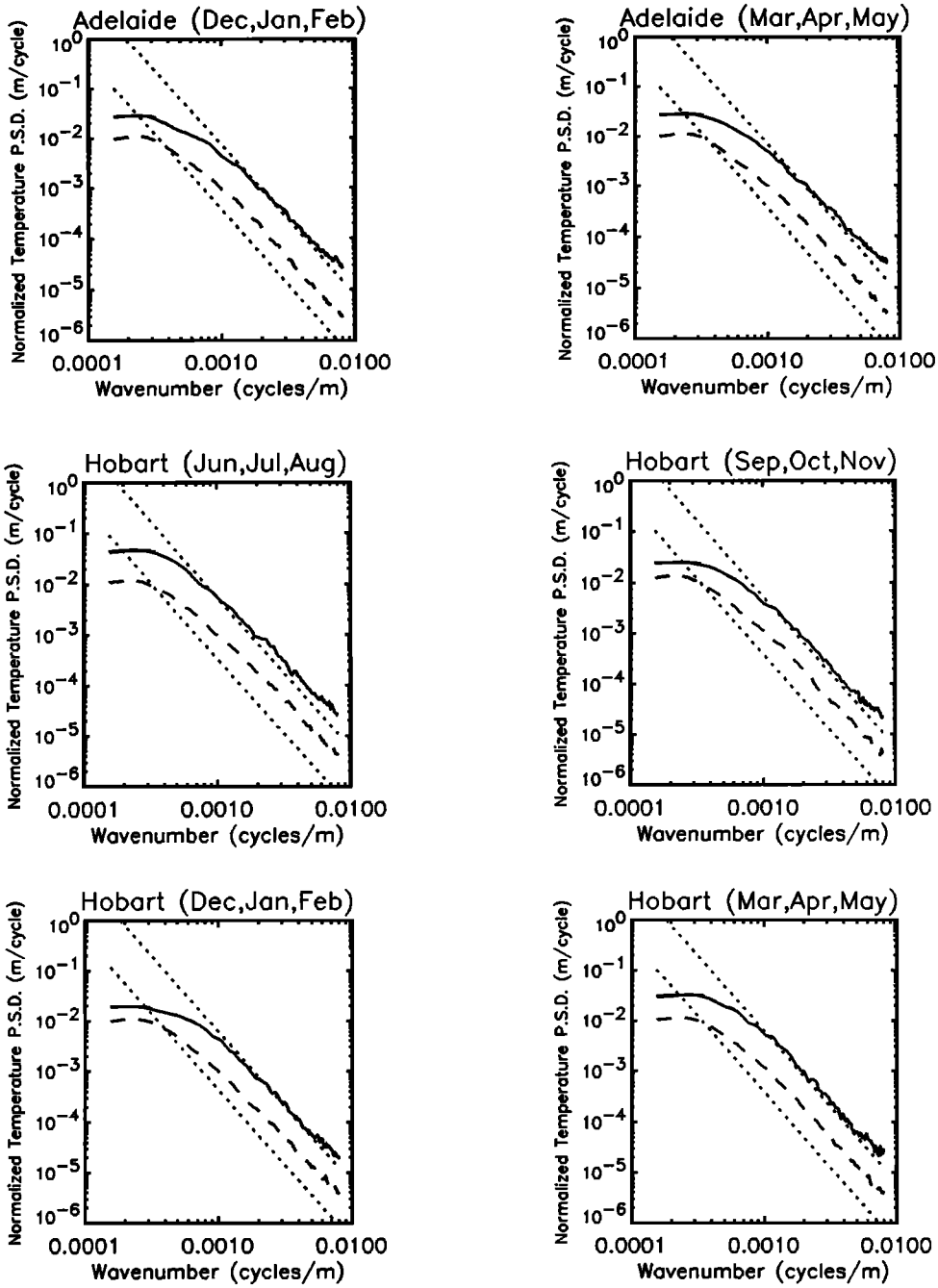

Figure 5. (continued)

Table 3 should be treated with some caution. More details about this problem are provided in the appendix, but it should be noted that estimates of other spectral parameters will not be affected.

The characteristic wavelength, $2\pi/m_*$, was found to be close to 2.5 km within both the troposphere and the lower stratosphere. Therefore the difference between characteristic phase speeds, c_*, within the two regions is determined mainly by differences in N. The gravity wave energy density is generally larger within the troposphere than the lower stratosphere, although observations from Gove, Darwin, and Willis Island provide exceptions.

The total gravity wave energy density, as estimated using (6), is chosen here as the measure for gravity wave activity. Time and latitude variations of the wave field are best studied using this parameter. Figure 7 displays contours of E_0 as a function of time and latitude for both the troposphere and the lower stratosphere. These were obtained by averaging the data into 1-month bins for six of the seven latitude bands that were described in Table 2. Data from Davis were not included since these were not available over the full 12-month period.

The energy densities of Figure 7 were calculated from the areas under monthly mean vertical wavenumber power spectra. Thus they refer to the total energy den-

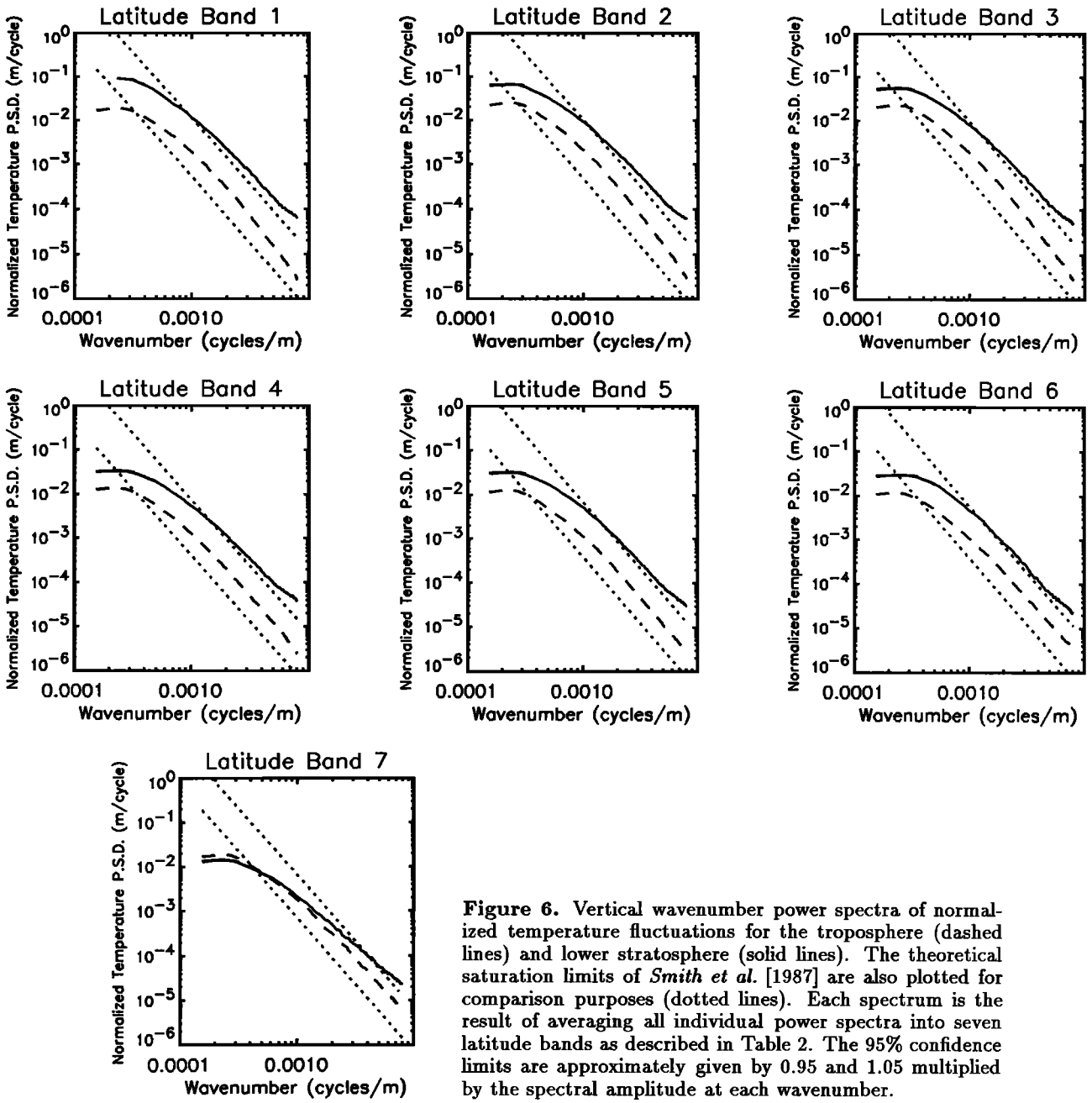

Figure 6. Vertical wavenumber power spectra of normalized temperature fluctuations for the troposphere (dashed lines) and lower stratosphere (solid lines). The theoretical saturation limits of *Smith et al.* [1987] are also plotted for comparison purposes (dotted lines). Each spectrum is the result of averaging all individual power spectra into seven latitude bands as described in Table 2. The 95% confidence limits are approximately given by 0.95 and 1.05 multiplied by the spectral amplitude at each wavenumber.

sity of waves within the 1.43×10^{-4} to 8.00×10^{-3} cycles per meter wavenumber range. Also, the raw 6 by 12 data array was rebinned using bilinear interpolation in order to obtain a smoother contour pattern. Therefore the resolution is greater than is justified from the original measurements.

Seasonal variations of stratosphere wave activity are easily recognized in Figure 7. These clearly confirm the seasonal trends described earlier which were inferred from the variations of power spectrum form. At low latitudes (10°S to 20°S) a clear annual variation is observed with wave energy peaking during the monsoon months of December to February. However, at middle latitudes (30°S to 40°S) a maximum is seen during the winter months when cold fronts sweep across southern Australia. A transition between these two regimes occurs at intermediate latitudes (20°S to 30°S) where a semiannual variation is observed.

The seasonal variations of troposphere wave activity are, surprisingly, not well correlated with those in the stratosphere. At middle latitudes (30°S to 40°S) a small peak in wave activity is seen during winter months but the variation is much smaller than that observed in the stratosphere. However, at lower latitudes (10°S to 30°S) a strong peak in energy density is observed between July and November which is in contrast with the stratosphere case where the maximum is found between December and February. This sudden increase in tropospheric wave energy does not coincide with particular meteorological events, nor can it be associated with any

Table 2. The Division of Stations Into Seven Latitude Bands

Latitude Band	Radiosonde Stations	Number of Profiles Analyzed	
		Stratosphere	Troposphere
1	Gove, Darwin	766	1086
2	Mt. Isa, Townsville, Port Hedland	1058	1373
3	Gladstone, Learmonth, Alice Springs	746	1083
4	Forrest, Woomera, Cobar, Lord Howe Island	1396	1806
5	Wagga, Albany, Adelaide	1252	1660
6	Hobart	452	799
7	Davis	435	481

one geographic feature since the maximum is seen at a number of different stations including Port Hedland, Alice Springs, Townsville, and Willis Island.

Latitudinal variations of gravity wave activity are evident in the contour plots of Figure 7. Generally, the yearly averaged energy density (Table 3) is found to decrease with latitude so that the highest values are observed at the low-latitude sites. This is particularly noticeable within the stratosphere, although it is less obvious at tropospheric heights. The trend can also be seen in the power spectra of Figure 6.

The variation of gravity wave energy density with height and time can be examined using the radiosonde data from each station. Figures 8, 9, and 10 present time-height contours of normalized temperature variance and total gravity wave energy density observed at Gove, Adelaide, and Davis which were chosen to represent low-, middle, and high-latitude sites, respectively. These were obtained by calculating the normalized temperature variance within 4-km intervals for each observed temperature profile which had continuous measurements up to at least 24 km. The measurements were then averaged into 1-month bins giving a 6 by 12 array of variance data. Finally, the energy densities were obtained using (6) and (7) and the contours were calculated after bilinear interpolation. Also plotted (Figures 11, 12, and 13) are the time-height contours of temperature and Vaisala-Brunt frequency squared from each station. These were included to provide details concerning the background atmosphere and have also been obtained by averaging the data into 4 km by 1 month bins.

The normalized temperature variances of Figures 8, 9, and 10 have been calculated by estimating $\overline{T}(z)$ with a fitted second-order polynomial. These are given by $\sum_{i=1}^{M}(\hat{T}'_i - \overline{\hat{T}'})^2/(M-1)$ for all i such that z_i is in the appropriate height range where $\hat{T}'_i = (T_i - \overline{T}(z_i))/\overline{T}(z_i)$ and where M is the number of data points that lie within this height range. Since the data are partitioned into 4 km height bins the energy densities refer to energy densities of gravity waves within the wavenumber range 2.5×10^{-4} cycles per meter to approximately 0.01 cycles per meter. Therefore they are not strictly comparable to the energy densities of Figure 7 since these refer to waves within a slightly larger wavenumber range.

The time-height contours of temperature observed at

Table 3. Spectral Parameter Estimates

Station	t		$m_*/2\pi$, Cycles per Meter		c_*, m s^{-1}		E_0, J kg^{-1}	
	Tr	St	Tr	St	Tr	St	Tr	St
Adelaide	2.8	2.5	3.8×10^{-4}	4.0×10^{-4}	4.7	9.0	5.7	4.5
Albany	2.8	2.6	3.8×10^{-4}	4.0×10^{-4}	4.7	9.0	6.0	4.5
Alice Springs	3.1	2.5	4.2×10^{-4}	3.7×10^{-4}	4.5	10.5	9.1	6.4
Cobar	3.0	2.5	4.1×10^{-4}	3.7×10^{-4}	4.4	9.9	6.5	4.9
Darwin	3.1	2.6	4.8×10^{-4}	4.2×10^{-4}	4.0	9.9	7.7	8.1
Davis	2.7	2.2	3.6×10^{-4}	3.3×10^{-4}	5.8	10.8	6.3	2.0
Forrest	3.0	2.4	4.3×10^{-4}	3.8×10^{-4}	4.2	9.7	6.5	4.6
Gladstone	3.0	2.5	4.0×10^{-4}	3.6×10^{-4}	4.8	10.9	8.0	6.4
Gove	3.0	2.5	4.5×10^{-4}	3.3×10^{-4}	4.3	12.5	6.6	9.8
Hobart	2.7	2.6	3.5×10^{-4}	4.1×10^{-4}	5.0	8.7	5.5	5.1
Learmonth	3.1	2.5	4.4×10^{-4}	3.9×10^{-4}	4.2	10.3	8.6	6.9
Lord Howe Island	2.9	2.4	4.2×10^{-4}	3.9×10^{-4}	4.3	9.5	5.6	3.9
Mount Isa	3.0	2.5	4.3×10^{-4}	3.7×10^{-4}	4.4	11.8	9.5	7.5
Port Hedland	3.1	2.5	4.6×10^{-4}	3.5×10^{-4}	3.9	11.4	10.5	7.1
Townsville	3.0	2.5	4.2×10^{-4}	4.0×10^{-4}	4.6	10.5	9.3	7.5
Wagga	2.8	2.5	3.7×10^{-4}	3.9×10^{-4}	4.7	9.3	5.8	5.0
Willis Island	3.0	2.5	4.5×10^{-4}	3.3×10^{-4}	4.3	12.3	7.2	8.4
Woomera	2.8	2.5	3.7×10^{-4}	3.9×10^{-4}	4.8	9.5	6.1	5.3

Tr = Troposphere, St = Stratosphere.

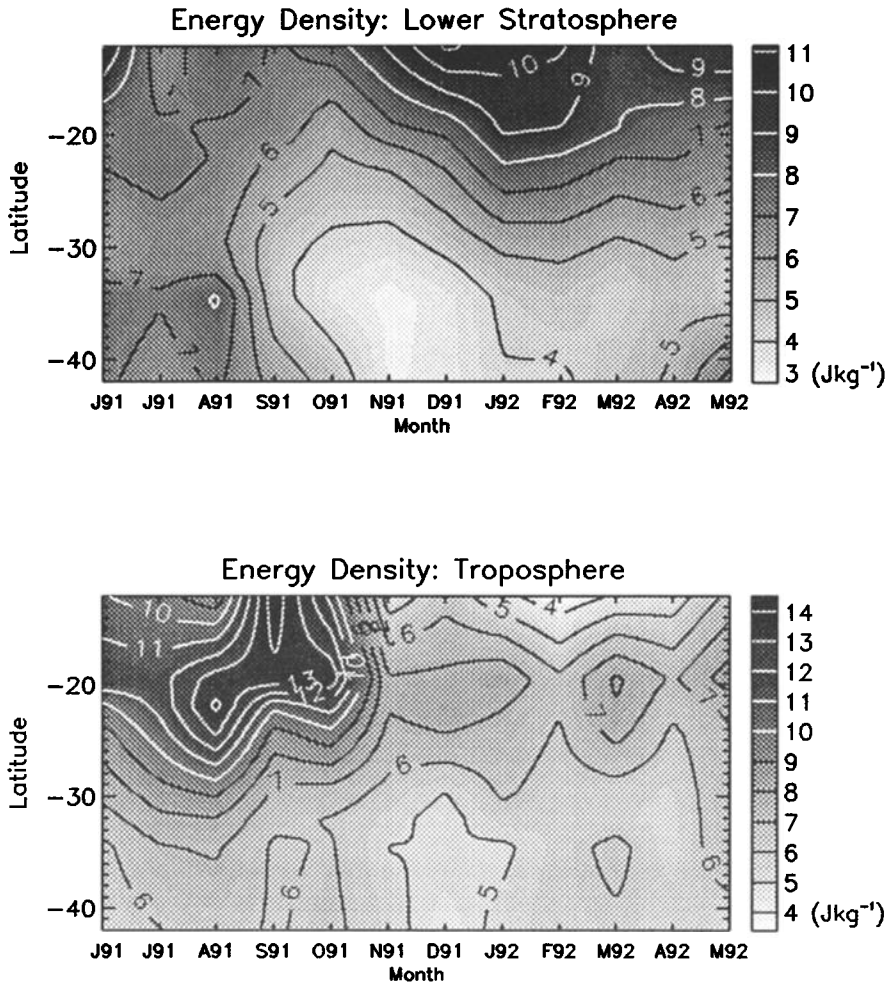

Figure 7. Time-latitude contours of total gravity wave energy density, E_0, for the troposphere and lower stratosphere. The energy density is calculated using (6) where $\overline{\hat{T}'^2}$ is the normalized temperature variance within the height intervals described in Table 1.

Gove (Figure 11) behave as expected showing a steady decrease in temperature from ground level until the tropopause is reached at approximately 17 km where the temperature begins to increase with height. There are no seasonal variations in the position of the tropopause or in the observed temperature gradients. The contours of Vaisala-Brunt frequency squared show a steplike increase at the tropopause with values in the stratosphere exceeding those of the troposphere by a factor of approximately 6. Here also there are no significant seasonal variations. The contours of gravity wave energy density tend to follow those of normalized temperature variance (Figure 8). In the troposphere, energy densities are of the order of 3 J kg^{-1}, although are generally larger between July and October, particularly at the lowest heights. This is in agreement with the seasonal variations described earlier. Once the tropopause is reached, however, the energy density is found to increase significantly taking values of the order of 10–16 J kg^{-1} at approximately 18 km. This rapid increase is followed by an equally rapid decrease near 20 km. However, the height range of measurements is not sufficient to determine the lowest value to which the energy density falls within the lower stratosphere.

Similar results are seen for the time-height contours of energy density observed at Adelaide and Davis. At Adelaide (Figure 9) a noticeable peak in wave energy density is found between 8 and 15 km, depending on the season. This follows the position of the tropopause as indicated by the contours of Vaisala-Brunt frequency squared (Figure 12). However, the peak in E_0 is not as large as the one found at Gove, nor is it as sharp. Notice also the large energy density values found within the lowest 4-km height bin. A discussion of these is left until the following section.

The contours of energy density observed at Davis (Figure 10) are particularly interesting in that a large peak is found at approximately 10 km between December 1992 and April 1993 but is not evident at this same height between July 1992 and December 1992. Referring to the contours of Vaisala-Brunt frequency squared (Figure 13), the period of December 1992 to April 1993 is characterized by a strong N^2 vertical gradient at 10 km. However, between July 1992 and December 1992

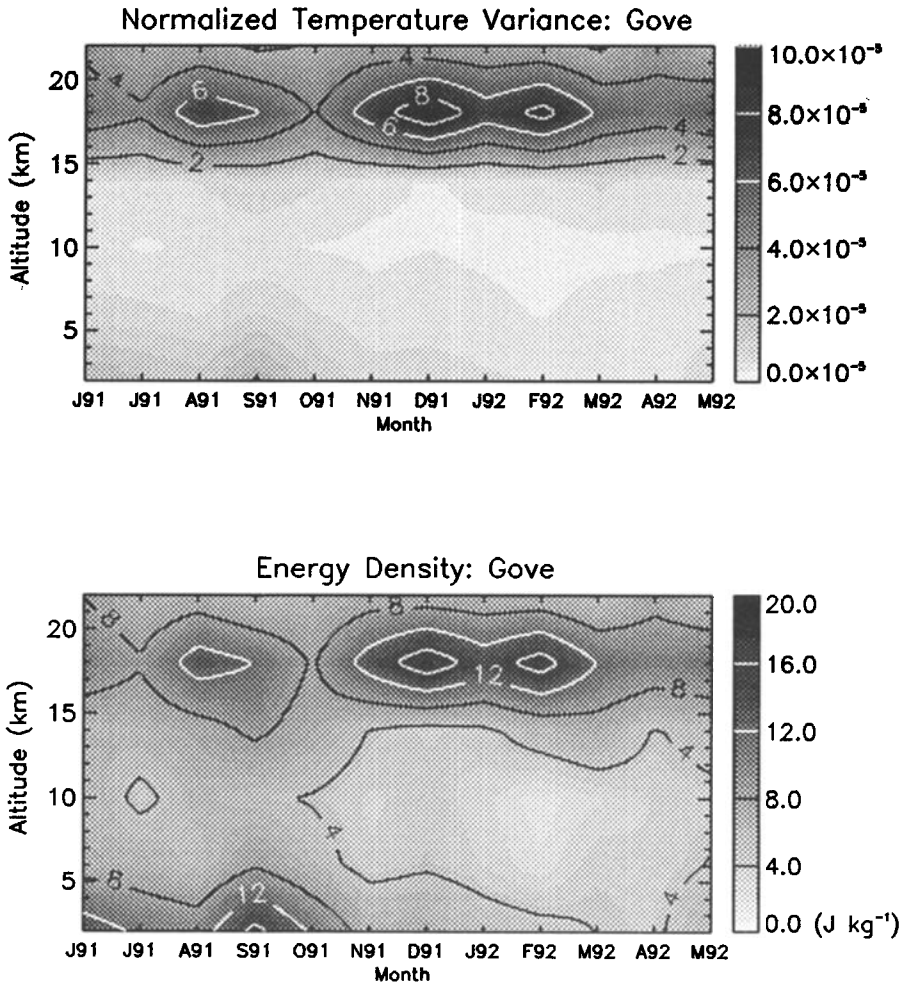

Figure 8. Time-height contours of normalized temperature variance and total gravity wave energy density observed at Gove between June 1991 and May 1992. The raw data have been interpolated to produce a smoother contour pattern.

this gradient is much weaker. Thus there is correlation between gravity wave energy density and the gradient of Vaisala-Brunt frequency squared within the vicinity of the tropopause. Also the energy density values within the lowest 4-km height bin are quite large, as was found to be the case at Adelaide.

5. Discussion

High-resolution radiosonde measurements made in the Australian sector of the southern hemisphere enable the variance of temperature to be investigated as a function of height, latitude, and season. The main results are given.

1. The vertical wavenumber power spectra have slopes that are close to −3 at most stations, especially within the troposphere.

2. There are clear seasonal variations of wave activity in the lower stratosphere (heights near 20 km) with the time of maximum activity changing from low-latitudes to midlatitudes. Seasonal variations of wave activity in the troposphere are, on the other hand, less clear.

3. Strong increases of normalized temperature variance are observed near the tropopause at times when there are large vertical gradients in atmosphere stability.

The observed power spectra within the stratosphere have high-wavenumber slopes that are slightly shallower than the theoretical expectation. This may result from a bias in estimates of temperature sensor response time as discussed in the appendix or from aliasing due to high spatial frequency noise. Furthermore, the sonde's horizontal drift will result in some distortion of the vertical wavenumber power spectra which are expected to have shallower slopes as a consequence [*Gardner and Gardner*, 1993]. All of these factors may be contributing to the spectral shape that is observed and so estimates of the spectral parameter t should not be regarded as inconsistent with the predicted −3 value within the stratosphere. The slopes of troposphere spectra, however, are in good agreement with theoretical expectations. These have not undergone the response time correction procedure as have those in the stratosphere and are less susceptible to problems associated with the

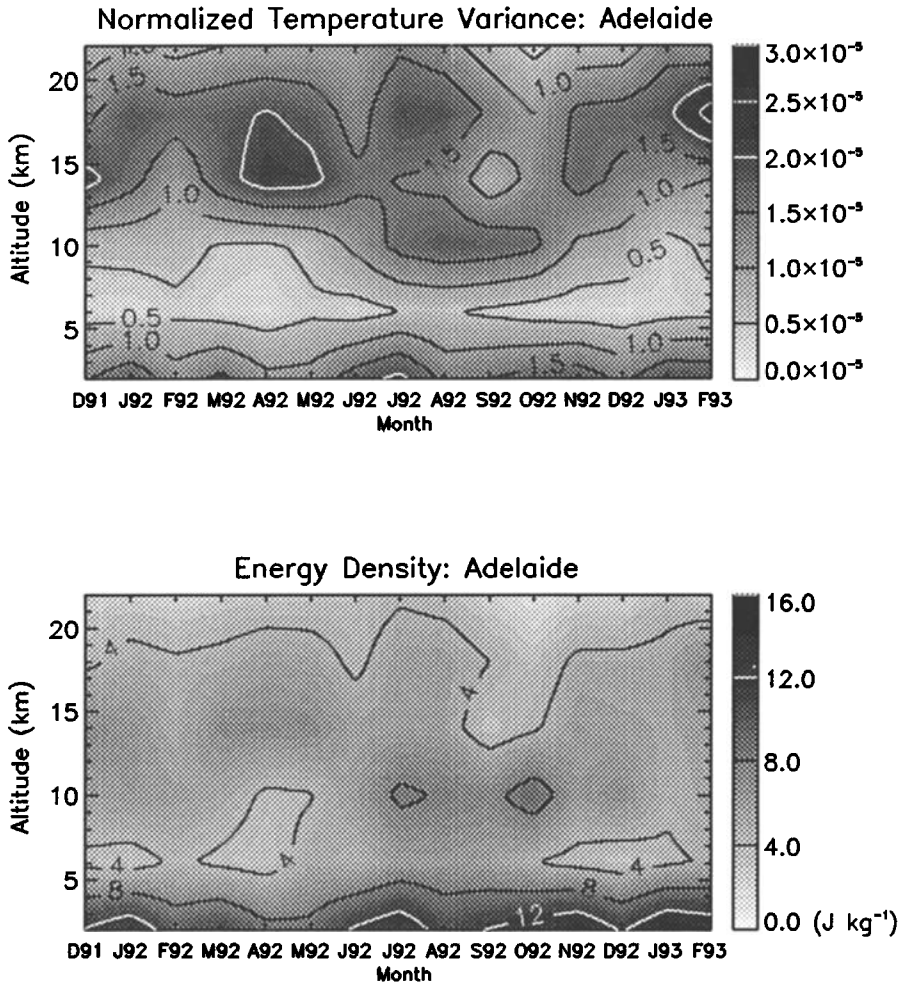

Figure 9. Time-height contours of normalized temperature variance and total gravity wave energy density observed at Adelaide between December 1991 and February 1993. The raw data have been interpolated to produce a smoother contour pattern.

sonde's drift since horizontal wind speeds tend to be weaker within the troposphere. Note, however, that the troposphere spectral amplitudes are larger than the gravity wave saturation limits of *Smith et al.* [1987].

It is often assumed that the small-scale temperature variations of the type discussed here are caused by gravity waves, an interpretation we have followed. While the vertical wavenumber spectral slopes are in the general range predicted by recent theories, the assumption that all temperature fluctuations are due to waves needs to be carefully examined, especially within the troposphere. Processes such as convection and inversions cause fluctuations on single profiles that are either difficult to distinguish from wave activity or difficult to remove from the background temperature profile. Both of these factors are likely to explain the large values of E_0 that are found within the lowest 4-km height bins of the time-height contour plots (Figures 8, 9, and 10). If some of the observed variance within these bins is not due to gravity waves then the values of E_0 will be overestimated. This may also explain the observed spectral amplitudes which are consistently larger in the troposphere than the theoretical gravity wave saturation limits of *Smith et al.* [1987]. A similar result was reported by *Tsuda et al.* [1991] after analysis of temperature profiles observed from Kyoto within a comparable height range.

The large increase of gravity wave energy density observed within the low-latitude troposphere (Figure 7) between July and November may also be explained in a similar manner. Low-altitude temperature inversions are more common at low latitudes during these months. As an example, Figure 2 shows the temperature profiles observed at Darwin between July 20 and July 29 and between January 20 and January 29. The profiles observed during July show strong temperature inversions between 1 and 3 km. Such strong inversions are less evident in the corresponding profiles from January. These inversions must contribute to the observed normalized temperature variance between 2.0 and 9.0 km during July and similar inversions are found at all other low-latitude stations. As a consequence, the total gravity wave energy density within the 2.0 to 9.0 km altitude range will be overestimated at these stations.

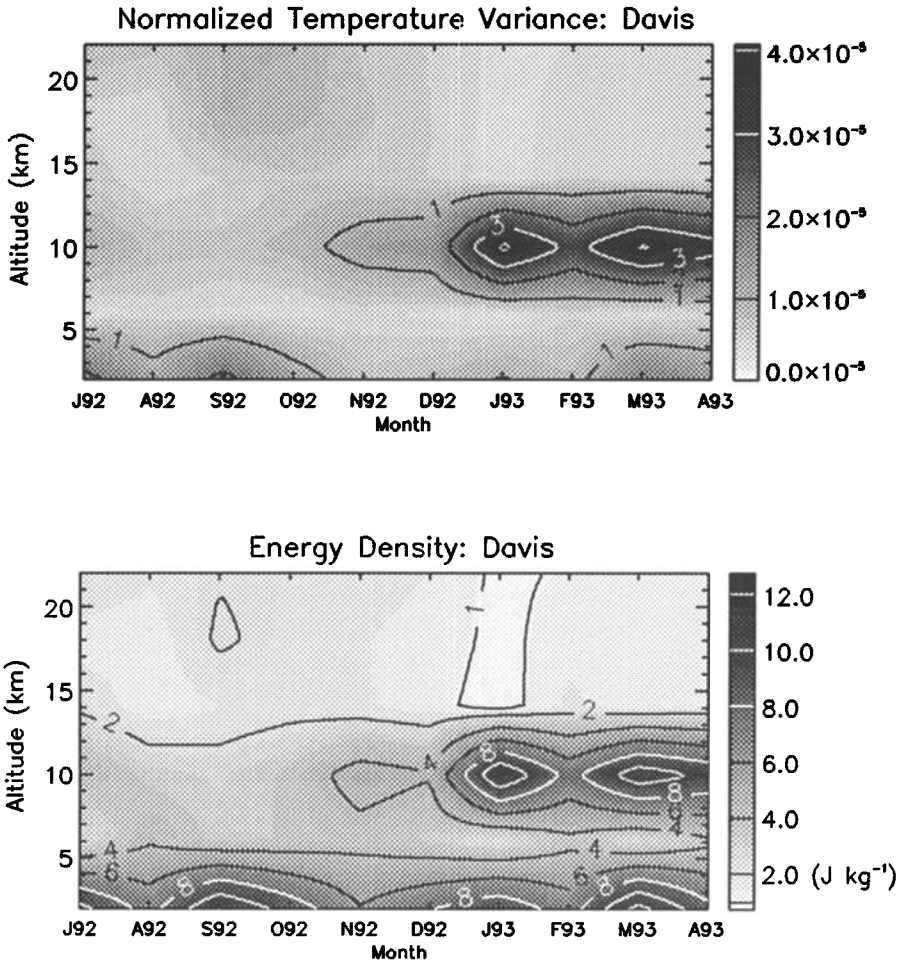

Figure 10. Time-height contours of normalized temperature variance and total gravity wave energy density observed at Davis between July 1992 and April 1993. The raw data have been interpolated to produce a smoother contour pattern.

Whether this is sufficient to explain the large increase described in Figure 7 is not known. Although they are not shown here, the power spectra calculated for both months are of similar shape but larger spectral amplitudes are found during July, particularly at the smallest vertical wavenumbers.

In the stratosphere it is more certain that small-scale temperature fluctuations are due to gravity waves. *Kitamura and Hirota* [1989], for example, show that the temperature and wind fluctuations in the lower stratosphere are consistent with the polarization relations of inertia-gravity waves. We find that, except for the Antarctic station of Davis, the stratospheric spectral amplitudes and slopes are generally consistent with theoretical expectations, and seasonal changes occur predominantly within the source-dependent region of the spectrum.

The spectral amplitudes in the stratosphere at Davis are interesting since they are smaller, particularly at the lowest vertical wavenumbers, than those observed at other stations. The spectral slopes are also more shallow than at other stations. In contrast, the spectral amplitudes within the troposphere are consistent with those found elsewhere which would appear to eliminate weak wave source activity as a cause. An alternative possibility is that the wave spectrum in the lower stratosphere is influenced in some way by the strong background zonal winds that are found over Davis (e.g., as proposed by *Fritts and Lu* [1993]). Generally, these are larger than at any other station studied in this paper. However, the zonal winds over Davis do show a strong seasonal variation with a maximum occurring during winter months. Therefore it would be reasonable to expect seasonal variations of the observed spectral amplitudes since the summer winds are comparable with those observed at other stations. Although they are not shown here, the observed spectra from the stratosphere over Davis show very little seasonal variation and the mean spectrum of Figure 6 is representative of the wave spectrum during all seasons. This appears to suggest that the interaction between the wave spectrum and the background zonal wind field is not responsible for the small spectral amplitudes and energy densities that are observed in the stratosphere over Davis. Our findings will be investigated further as information from other Antarctic stations becomes available.

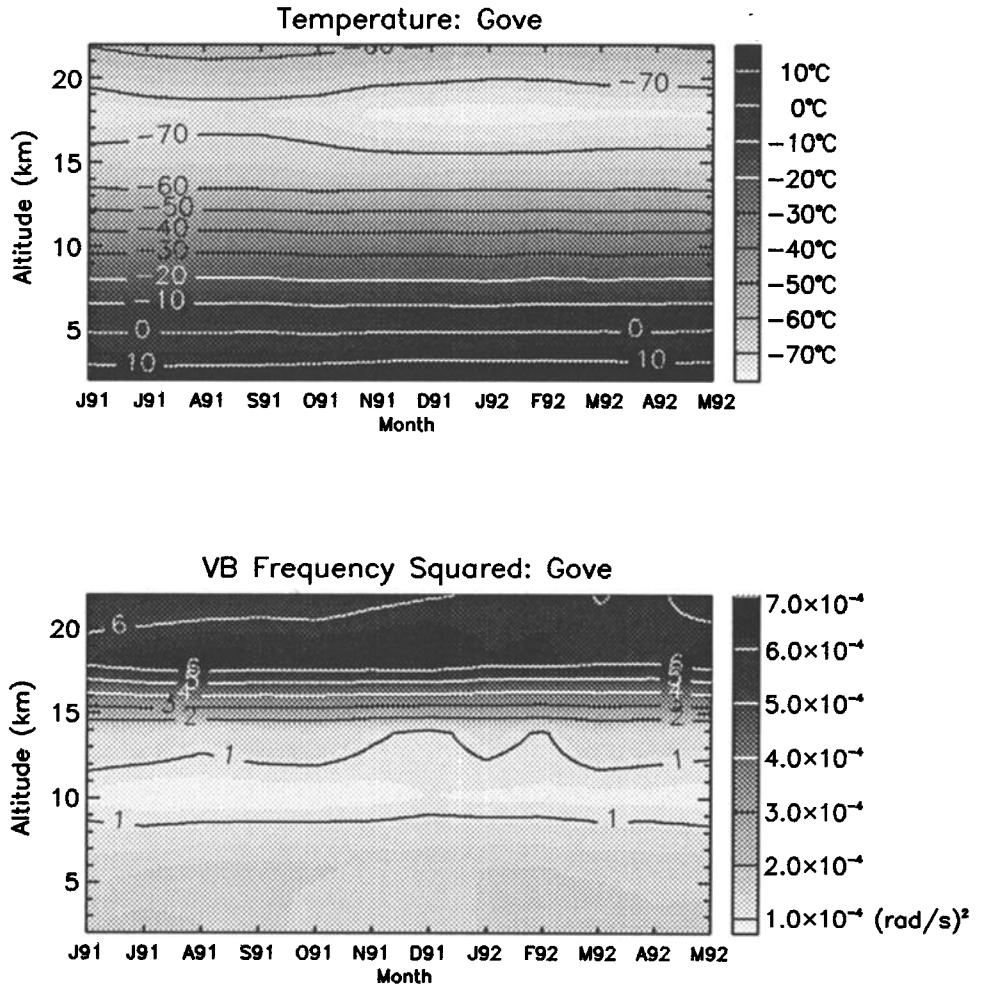

Figure 11. Time-height contours of temperature and Vaisala-Brunt frequency squared observed at Gove between June 1991 and May 1992. The raw data have been interpolated to produce a smoother contour pattern.

Figure 14 summarizes the seasonal and latitudinal variations of normalized temperature variance and E_0 at heights near 20 km. The error bars indicate the 95% confidence limits of estimates from each latitude band. This diagram, together with Figure 7, emphasizes the annual cycle in wave activity at low latitudes which is out-of-phase with wave activity at midlatitudes. In all seasons, but especially in summer, there is a strong equatorward gradient in energy density, with E_0 increasing by a factor of about 5 from polar to equatorial latitudes. These results agree well with other studies in the northern hemisphere. *Kitamura and Hirota* [1989] found that wave activity in the midlatitude lower stratosphere over Japan maximized in winter, and that wave activity increased toward the equator. Lidar studies at altitudes of 35 km over western Europe also show an annual cycle of temperature variability with a winter maximum and an equatorward gradient in the temperature fluctuations [*Souprayen*, 1993].

It is possible that Kelvin waves or other equatorially trapped waves have made sizeable contributions to the normalized temperature variances that were observed at low-latitude sites. Without wind velocity measurements, however, it is impossible to study the polarization of waves, and we are therefore unable to determine the significance of this contribution.

It should be noted that E_0 is the measure of wave activity used in the *Fritts and VanZandt* [1993] parameterization scheme. However, other schemes may use different indicators of wave activity. In some cases these parameters can still be estimated from our figures and tables. For example, C. O. Hines (private communication, 1994) has developed a scheme which uses the root-mean-square of the horizontal wind perturbation as the input parameter. This may be estimated from normalized temperature variance measurements using the following equation,

$$\overline{V_H'^2} = \overline{u'^2} + \overline{v'^2} \approx \frac{pg^2}{N^2}\overline{\hat{T}'^2} \tag{14}$$

where V_H' is the first-order perturbation of total horizontal wind velocity. Equation (14) is derived from standard polarization equations by assuming that the spectrum of waves is separable in all variables and that

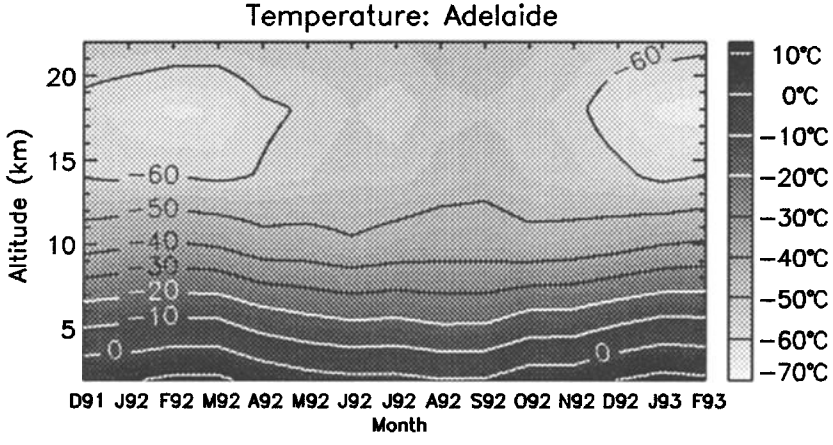

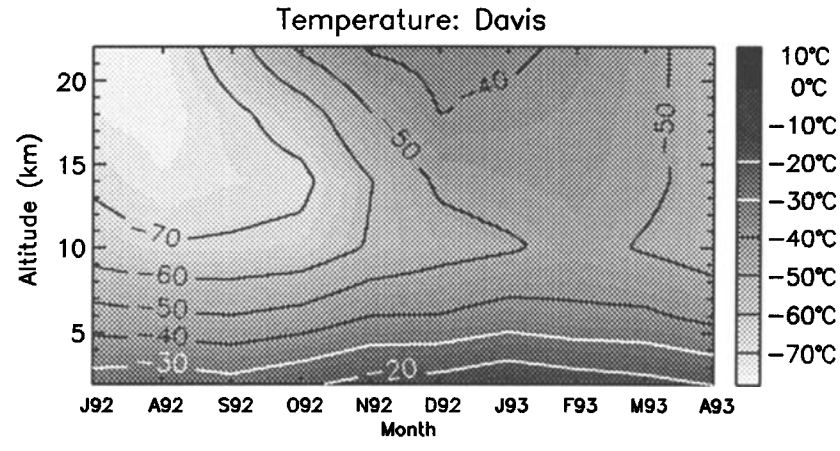

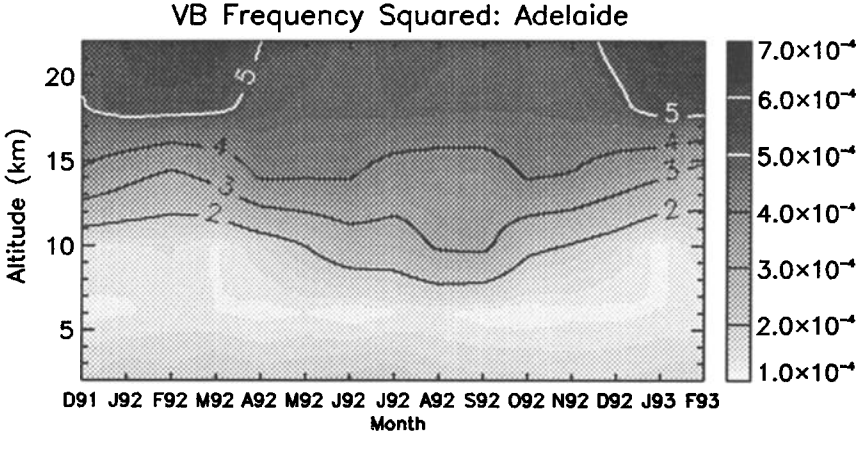

Figure 12. Time-height contours of temperature and Vaisala-Brunt frequency squared observed at Adelaide between December 1991 and February 1993. The raw data have been interpolated to produce a smoother contour pattern.

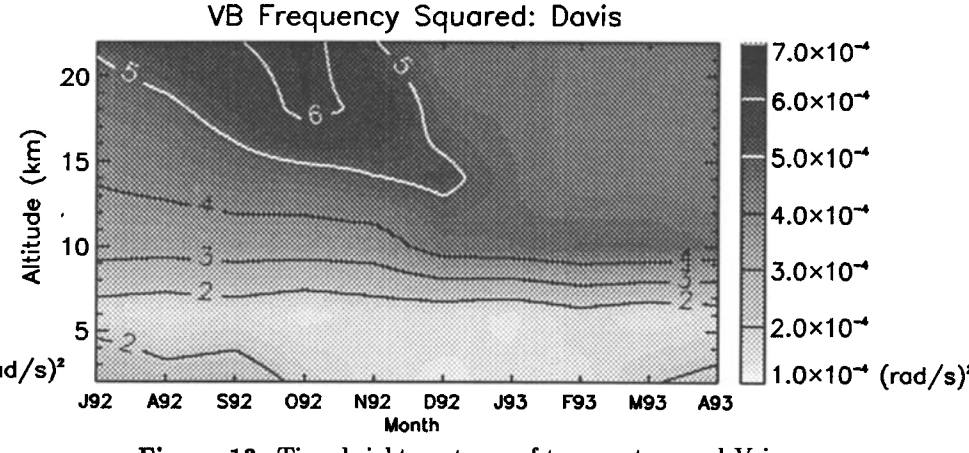

Figure 13. Time-height contours of temperature and Vaisala-Brunt frequency squared observed at Davis between July 1992 and April 1993. The raw data have been interpolated to produce a smoother contour pattern.

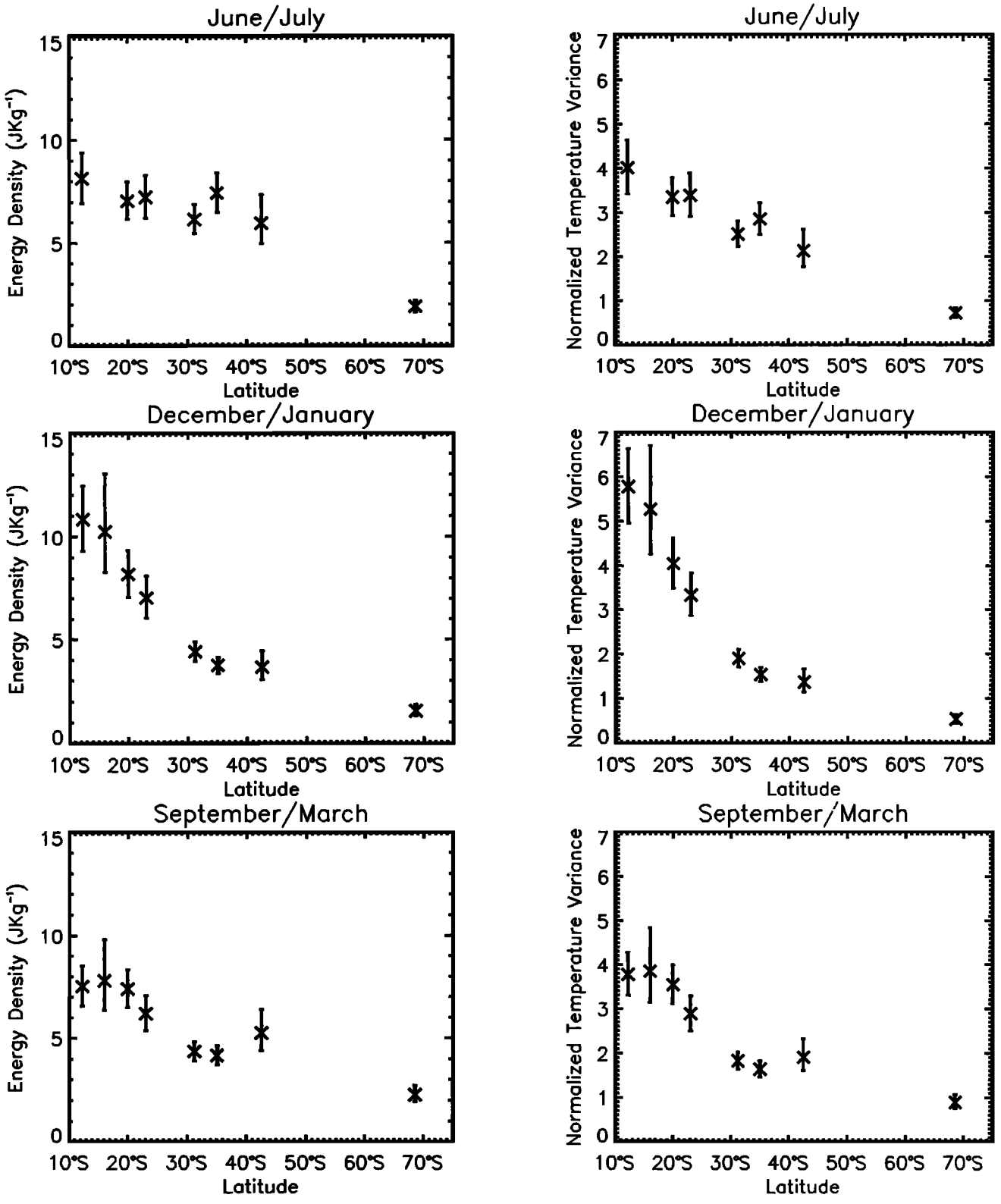

Figure 14. The variation of normalized temperature variance and gravity wave energy density as a function of latitude within the lower stratosphere (17.0 to 24.0 km in most cases). Data from the various stations have been averaged into latitude bands as described in Table 2 and over 2-month periods in each case. Furthermore, the results from Willis Island are included for the months of December/January and September/March. Normalized temperature variance estimates have been multiplied by a factor of 10^5 and error bars indicate the 95% confidence limits of each estimate.

the one-dimensional frequency spectrum is given by $B(\omega) \propto \omega^{-p}$. From Figure 14 and using $p = 5/3$ it can be seen that the root-mean-square of V'_H varies from approximately 1.5 m s^{-1} at Davis to approximately 4.0 m s^{-1} at 10°S.

The local increases in temperature variance and E_0 at the tropopause are interesting features which must also be treated with caution. They may be artifacts due to the high-pass filtering of the temperature profiles in the presence of the sharp gradients at the tropopause. However, we believe that this contribution is not great. To demonstrate this a simulated background temperature profile, $\overline{T}(z)$, was sampled at 50-m intervals over a 4 km height range. For the first 2 km of this range the profile was given by a straight line with a gradient of −6°C per kilometer and for the last 2 km by a straight line with a gradient of 2°C per kilometer. Thus the tropopause was simulated as an abrupt kink in the profile at a position of exactly halfway along the given 4 km height range. This represents an extreme example since the transition is rarely observed to be this sharp. By fitting a second-order polynomial, also sampled at 50-m intervals, to the simulated background profile, it is possible to calculate a normalized temperature variance in the usual manner. This simulates the contribution to the variance from the tropopause in an extreme case. We calculated the normalized temperature variance to be 7.4×10^{-6}. This may then be compared with the observed peak variances at Davis ($\approx 3.5 \times 10^{-5}$), Adelaide ($\approx 2.0 \times 10^{-5}$), and Gove ($\approx 8.0 \times 10^{-5}$) which suggests that the method of analysis is not significantly influencing these results.

The enhancements of wave energy density near the tropopause may be indicative of gravity wave "supersaturation" in this region. *VanZandt and Fritts* [1989] proposed that vertically propagating waves, upon encountering a sudden increase in atmosphere stability, will have larger than saturation amplitudes over a distance of approximately one vertical wavelength. This arises due to the N dependence of vertical wavenumber as defined by the gravity wave dispersion relation. Furthermore, the energy that is dissipated as waves return to their saturation amplitudes can result in enhanced wave drag provided that the spectrum of waves is azimuthally anisotropic [*VanZandt and Fritts*, 1989]. The "supersaturation" hypothesis as well as other possible explanations for these results will be discussed elsewhere.

6. Conclusions

A climatological study of gravity wave activity based on a data set of high-resolution radiosonde measurements has been presented. The utility of radiosonde data in gravity wave studies has also been investigated in some detail. It was found that the radiosonde temperature sensor's slow response at stratospheric heights can cause significant spectral distortion at high vertical wavenumbers. A correction technique was developed to address this concern.

The advantage of using radiosonde measurements for gravity wave research is their extensive geographic and temporal coverage. This allows estimates of important spectral parameters to be made which are not biased by localized source effects. It also allows seasonal and latitudinal variations of gravity wave activity to be identified. Inspection and comparison of stratosphere power spectra indicate that most of the variations occur at low vertical wavenumbers. The stratosphere spectral amplitudes at high wavenumbers, with the exception of those observed at Davis, are generally consistent with the theoretical saturation limits proposed by *Smith et al.* [1987]. Variations of the gravity wave spectral form within the troposphere are more difficult to interpret. These results are likely to be contaminated by convection and temperature inversions.

Climatological studies of gravity waves are important in defining the extent of wave activity throughout the atmosphere. If theorists and modelers believe that more work of this nature is needed within the lower atmosphere then a global-scale study of radiosonde data will provide an important contribution. All that is needed is for certain stations throughout the world, which are already launching radiosondes on a daily basis, to archive their data at high resolution. However, it should be noted that temperature measurements alone are not sufficient to fully describe the gravity wave field. In particular, the degree of wave field anisotropy is an important parameter which requires wind velocity measurements in order to be estimated.

Appendix: Temperature Sensor Response Time

The temperature sensor response times that have been used in obtaining the corrected stratosphere power spectra have themselves been estimated from the results presented in two Vaisala Oy test reports [*Turtiainen*, 1991a,b]. According to *Turtiainen* [1991b], the response time τ of a temperature sensor in a flowing gas is theoretically given by

$$\tau = C_1 + C_2/h \qquad \text{(A1)}$$

where h is the surface heat transfer coefficient and where C_1 and C_2 are constants that depend upon the sensor dimensions and materials. This result has been obtained from *Kerlin et al.* [1982]. The surface heat transfer coefficient is a complicated function of sensor ventilation speed, air density, and air temperature [*Turtiainen*, 1991b], and the height dependence of τ follows from this term. Thus if C_1 and C_2 are known for a given type of sensor then τ can be computed theoretically at any height providing that T, ρ, and the sensor's ventilation speed are known.

The constants C_1 and C_2 were estimated by *Turtiainen* [1991b] for the Vaisala RS80–15 temperature sensor. This was achieved by experimentally determining the response time at ground level conditions for three different ventilation speeds. Thus τ was known

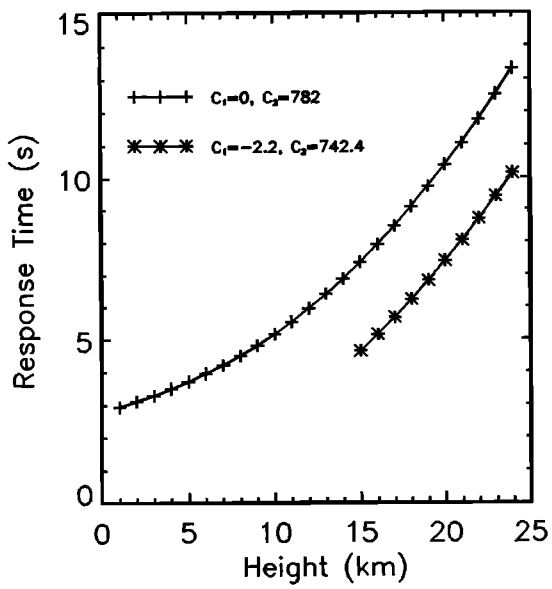

Figure 15. The height dependence of temperature sensor response time for different values of C_1 and C_2 (see text for more details). The response time was calculated using (A1) where the surface heat transfer coefficient, a function of temperature and density, was determined using the mean temperature and pressure profiles observed at Adelaide during December 1991.

for three values of h allowing C_1 and C_2 to be estimated by least squares curve fitting. The values were found to be $C_1 \approx 0$ and $C_2 = 782$. Note that the response time was experimentally determined by measuring the time taken for the sensor to reach 63.2% of a sudden step function increase of environment temperature. Figure 15 displays the height dependence of τ where (A1) has been used and where h was determined using the mean temperature and pressure profiles observed at Adelaide during December 1991. Atmosphere density was calculated from the temperature and pressure measurements using the ideal gas equation and the sensor ventilation rate was taken to be equivalent to the mean balloon ascent velocity.

In the work by *Turtiainen* [1991a, p. 5] temperature sensor response times were measured using a radiosonde in flight where the step function increase in environment temperature was generated using a heating element attached to the sonde. The results, however, were consistently smaller than the corresponding theoretical values which were calculated using C_1 and C_2 given above. This leads to the conclusion of the report which states that "the response time of RS80 temperature sensor in flight was found to be equal or less than the theoretically computed values presented in the earlier reports." Thus it appears that (A1) with $C_1 = 0$ and $C_2 = 782$ is overestimating the temperature sensor response time within the lower stratosphere given that all measurements by *Turtiainen* [1991a] were made at pressures that were less than or equal to 44 hPa.

As a result of the above problem we believe that it is more appropriate to find C_1 and C_2 for the stratosphere by fitting (A1) to the results presented by *Turtiainen* [1991a]. We have done this for the 12 measurements of response time τ that are given in this report and have been made at various different pressures, temperatures, and ventilation speeds. The parameters were found to be $C_1 = -2.2$ and $C_2 = 724.4$ and the height dependence of τ using these parameters has been plotted in Figure 15 where h was determined, as before, from the mean pressure and temperature profiles observed at Adelaide during December 1991. Clearly, this new curve is not strictly valid near ground level since it underestimates the ground level measurements of τ. Nevertheless, it does provide a superior fit to those measurements of τ that have been made within the stratosphere.

The corrections to the observed power spectra of this study have been calculated using (12) where τ was found from (A1) with $C_1 = -2.2$ and $C_2 = 724.4$. This leads to height-averaged response times that are of the order of 7 to 8 s within the 17 to 24 km altitude range and 1 to 2 s within the 2 to 9 km altitude range. The value of τ between 2 and 9 km is no doubt an underestimate of the true value within this height interval. However, this is not important since even when the parameters $C_1 = 0$ and $C_2 = 782$ are used, the response time is still sufficiently small that the correction for tropospheric power spectra is negligible at all but the very highest wavenumbers. Consequently, all observed tropospheric vertical wavenumber power spectra have not been altered in any way.

The method that has been chosen in order to obtain values for the parameters C_1 and C_2 is not the only plausible procedure. Given the available information, however, we believe that it provides the best estimates of τ within the lower stratosphere. Nevertheless, our approach may result in nonnegligible errors for the response time estimates. These are difficult to quantify and will affect the high-wavenumber spectral slope, t, of corrected power spectra which, as a consequence, may be biased in some way. It is important to note, however, that the spectral parameters m_*, c_*, and E_0 will not be significantly affected by this problem. As a result, only estimates of t from stratosphere power spectra need be treated with some caution.

Another possible source of error for corrected vertical wavenumber power spectra arises due to the assumption that τ is constant in obtaining (12). Figure 15 indicates that τ is not constant within the height intervals of interest to this study. However, (12) is still valid to good approximation if height-averaged response times are used. To demonstrate this a normalized temperature fluctuation profile has been numerically simulated for altitudes between 17 and 24 km. This was obtained by summing a series of sinusoids with amplitudes that were determined from a standard gravity wave model and by applying the constraints imposed due to the slow response of the radiosonde's temperature sensor.

The fluctuation profile was simulated by first generating a model gravity wave power spectrum using (13) with $F_0/2\pi = 0.05$ m/cycle, $m_*/2\pi = 5.0 \times 10^{-4}$ cy-

cles/m and $t = 3$. A series of 100 sinusoids was then calculated at wavenumbers $m_i = 2\pi \times 10^{-4} i$ where i is an integer between 1 and 100 and where each sinusoid has been assigned a random phase ϕ. The amplitudes, $A_i(m_i)$, were determined from the model spectrum since these are given by the square root of twice the variance within the relevant wavenumber band about wavenumber m_i. The summation of individual sinusoids, sampled at 7-m altitude intervals between 16 and 24 km, gives the simulated environment fluctuation profile. This technique follows the work of *Eckermann* [1990].

The fluctuation profile measured by a radiosonde with temperature sensor response time τ is related to the environment fluctuation profile according to (10) where T and T_s may be replaced by $\hat{T}'$ and $\hat{T}_s'$, respectively, assuming $\overline{T_s}(z)$ does not differ significantly from $\overline{T}(z)$ and assuming $\overline{T}(z)$ is approximately constant over the altitude range of interest. However, if τ is variable in height then (10) cannot be solved analytically. The simulated fluctuation profile was thus obtained using the Runge-Kutta method where $\tau(z)$ was given by the curve of Figure 15 defined by $C_1 = -2.2$ and $C_2 = 742.4$. The first kilometer of data was discarded in order to allow sufficient altitude for any transient effects to become negligible. Thus the final simulated profile comprised data that was sampled at 7-m intervals between 17 and 24 km.

The simulated fluctuation profile was spectrally analyzed using the Blackman-Tukey algorithm and was further modified using (12) where τ was given by the height-averaged response time between 17 and 24 km. Although not shown here, the resultant power spectrum was found to be in good agreement with the original model spectrum. This indicates that (12) is valid to good approximation over 7-km altitude intervals if τ is given by its height-averaged value.

Acknowledgments. The provision of data by the National Climate Centre, Australian Bureau of Meteorology is gratefully acknowledged. We also thank S. K. Avery, S. D. Eckermann, W. K. Hocking, T. Tsuda, and T. E. VanZandt for their helpful suggestions and/or careful reading of earlier versions of the manuscript. This work is supported by the Australian Research Council and S.J.A. acknowledges the support of an Australian Postgraduate Research Award.

References

Bath, M., *Spectral Analysis in Geophysics*, vol. 7, *Developments in Solid Earth Geophysics*, Elsevier Science, New York, 1974.

Cot, C., and J. Barat, A "universal" wave spectrum for atmospheric temperature and velocity fluctuations in the stratosphere?, *Geophys. Res. Lett., 17*, 1577–1580, 1990.

Dewan, E. M., Stratospheric wave spectra resembling turbulence, *Science, 204*, 832–835, 1979.

Dewan, E. M., and R. E. Good, Saturation and the "universal" spectrum for vertical profiles of horizontal scalar winds in the atmosphere, *J. Geophys. Res., 91*, 2742–2748, 1986.

Dewan, E. M., N. Grossbard, A. F. Quesada, and R. E. Good, Spectral analysis of 10 m resolution scalar velocity profiles in the stratosphere, *Geophys. Res. Lett., 11*, 80–83, 1984. (Correction, *Geophys. Res. Lett., 11*, 624, 1984.)

Eckermann, S. D., Effects of nonstationarity on spectral analysis of mesoscale motions in the atmosphere, *J. Geophys. Res., 95*, 16685–16703, 1990.

Eckermann, S. D., and R. A. Vincent, VHF radar observations of gravity-wave production by cold fronts over southern Australia, *J. Atmos. Sci., 50*, 785–806, 1993.

Eckermann, S. D., I. Hirota, and W. K. Hocking, Gravity wave and equatorial wave morphology of the stratosphere derived from long-term rocket soundings, *Q. J. R. Meteorol. Soc.*, in press, 1994.

Ferraz-Mello, S., Estimation of periods from unequally spaced observations, *Astron. J., 86*, 619–624, 1981.

Fritschen, L. J., and L. W. Gay, *Environmental Instrumentation*, Springer-Verlag, New York, 1979.

Fritts, D. C., and W. Lu, Spectral estimates of gravity wave energy and momentum fluxes, II, Parameterization of wave forcing and variability, *J. Atmos. Sci., 50*, 3695–3713, 1993.

Fritts, D. C., and G. D. Nastrom, Sources of mesoscale variability of gravity waves, II, Frontal, convective, and jet stream excitation, *J. Atmos. Sci., 49*, 111-127, 1992.

Fritts, D. C., and T. E. VanZandt, Spectral estimates of gravity wave energy and momentum fluxes, I, Energy dissipation, acceleration, and constraints, *J. Atmos. Sci., 50*, 3685–3694, 1993.

Fritts, D. C., T. Tsuda, T. Sato, S. Fukao, and S. Kato, Observational evidence of a saturated gravity wave spectrum in the troposphere and lower stratosphere, *J. Atmos. Sci., 45*, 1741–1759, 1988.

Fritts, D. C., T. Tsuda, T. E. VanZandt, S. A. Smith, T. Sato, S. Fukao, and S. Kato, Studies of velocity fluctuations in the lower atmosphere using the MU radar, II, Momentum fluxes and energy densities, *J. Atmos. Sci., 47*, 51–66, 1990.

Gage, K. S., Evidence for a $k^{5/3}$ power law inertial range in mesoscale two-dimensional turbulence, *J. Atmos. Sci., 36*, 1950–1954, 1979.

Gage, K. S., and G. D. Nastrom, On the spectrum of atmospheric velocity fluctuations seen by MST/ST radar and their interpretation, *Radio Sci., 20*, 1339–1347, 1985.

Gardner, C. S., and N. F. Gardner, Measurement distortion in aircraft, space shuttle, and balloon observations of atmospheric density and temperature perturbation spectra, *J. Geophys. Res., 98*, 1023–1033, 1993.

Gossard, E. E., and W. H. Hooke, *Waves in the Atmosphere*, Elsevier Science, New York, 1975.

Hamilton, K., Climatological statistics of stratospheric inertia-gravity waves deduced from historical rocketsonde wind and temperature data, *J. Geophys. Res., 96*, 20831–20839, 1991.

Hines, C. O., The saturation of gravity waves in the middle atmosphere, II, Development of Doppler-spread theory, *J. Atmos. Sci., 48*, 1360–1379, 1991.

Hines, C. O., Pseudosaturation of gravity waves in the middle atmosphere: An interpretation of certain lidar observations, *J. Atmos. Terr. Phys., 55*, 441–445, 1993.

Kerlin, T. W., R. L. Shepard, H. M. Hashemian, and K. M. Petersen, *Response of Installed Temperature Sensors. Temperature, Its Measurement and Control in Science and Industry*, vol. 5, American Institute of Physics, New York, 1982.

Kitamura, Y., and I. Hirota, Small-scale disturbances in the lower stratosphere revealed by daily rawin sonde observations, *J. Meteorol. Soc. Jpn., 67*, 817–830, 1989.

Lilly, D. K., Stratified turbulence and the mesoscale vari-

ability of the atmosphere, *J. Atmos. Sci., 40*, 749–761, 1983.

Nastrom, G. D., and D. C. Fritts, Sources of mesoscale variability of gravity waves, I, Topographic excitation, *J. Atmos. Sci., 49*, 101–110, 1992.

Sawyer, J. S., Quasi-periodic wind variations with height in the lower stratosphere, *Q. J. R. Meteorol. Soc., 87*, 24–33, 1961.

Senft, D. C., C. A. Hostetler, and C. S. Gardner, Characteristics of gravity wave activity and spectra in the upper stratosphere and upper mesosphere at Arecibo during early April 1989, *J. Atmos. Terr. Phys., 55*, 425–439, 1993.

Sidi, C., J. Lefrere, F. Dalaudier, and J. Barat, An improved atmospheric buoyancy wave spectrum model, *J. Geophys. Res., 93*, 774–790, 1988.

Smith, S. A., D. C. Fritts, and T. E. VanZandt, Evidence for a saturated spectrum of atmospheric gravity waves, *J. Atmos. Sci., 44*, 1404–1410, 1987.

Souprayen, C., Climatologie des ondes de gravite dans l'atmosphere moyenne: Contribution a leur parametrisation dans les modeles numiriques, Ph.D. thesis, l'Univ. Pierre et Marie Curie Paris, 1993.

Thompson, R. O. R. Y., Observation of inertial waves in the stratosphere, *Q. J. R. Meteorol. Soc., 104*, 691–698, 1978.

Tsuda, T., T. Inoue, D. C. Fritts, T. E. VanZandt, S. Kato, T. Sato, and S. Fukao, MST radar observations of a saturated gravity wave spectrum, *J. Atmos. Sci., 46*, 2440–2447, 1989.

Tsuda, T., T. E. VanZandt, M. Mizumoto, S. Kato, and S. Fukao, Spectral analysis of temperature and Brunt-Vaisala frequency fluctuations observed by radiosondes, *J. Geophys. Res., 96*, 17265–17278, 1991.

Turtiainen, H., Response time of RS80 temperature sensor in flight, technical report, Vaisala Oy, Finland, 1991a.

Turtiainen, H., Response time test of Vaisala RS80 temperature sensor, technical report, Vaisala Oy, Finland, 1991b.

VanZandt, T. E., A universal spectrum of buoyancy waves in the atmosphere, *Geophys. Res. Lett., 9*, 575–578, 1982.

VanZandt, T. E., and D. C. Fritts, A theory of enhanced saturation of the gravity wave spectrum due to increases in atmospheric stability, *Pure Appl. Geophys., 130*, 399–420, 1989.

Vincent, R. A., and S. D. Eckermann, VHF radar observations of mesoscale motions in the troposphere: Evidence for gravity wave Doppler shifting, *Radio Sci., 25*, 1019–1037, 1990.

Weinstock, J., Saturated and unsaturated spectra of gravity waves and scale dependent diffusion, *J. Atmos. Sci., 47*, 2211–2225, 1990.

Wilson, R., M. L. Chanin, and A. Hauchecorne, Gravity waves in the middle atmosphere observed by Rayleigh lidar, 2, Climatology, *J. Geophys. Res., 96*, 5169–5183, 1991.

S. J. Allen and R. A. Vincent, Department of Physics and Mathematical Physics, University of Adelaide, Adelaide, South Australia, 5005, Australia. (e-mail: sallen@physics.adelaide.edu.au; rvincent@physics.adelaide.edu.au)

(Received March 11, 1994; revised June 9, 1994; accepted July 9, 1994.)